

1
2
3
4
5
6
7
8
9
10
11
12
13
14
15
16
17
18

Endemic means change as SARS-CoV-2 evolves

Sarah P. Otto¹, Ailene MacPherson², & Caroline Colijn²

1. Department of Zoology & Biodiversity Research Centre, University of British Columbia, Vancouver, BC V6T 1Z4, Canada. otto@zoology.ubc.ca
2. Department of Mathematics, Simon Fraser University, Burnaby, BC V5A 1S6, Canada

19 **Summary**

20 COVID-19 has become endemic, with dynamics that reflect the waning of immunity and re-exposure,
21 by contrast to the epidemic phase driven by exposure in immunologically naïve populations. Endemic
22 does not, however, mean constant. Further evolution of SARS-CoV-2, as well as changes in behaviour
23 and public health policy, continue to play a major role in the endemic load of disease and mortality. In
24 this paper, we analyse evolutionary models to explore the impact that newly arising variants can have on
25 the short-term and longer-term endemic load, characterizing how these impacts depend on the
26 transmission and immunological properties of variants. We describe how evolutionary changes in the
27 virus will increase the endemic load most for persistently immune-escape variants, by an intermediate
28 amount for more transmissible variants, and least for transiently immune-escape variants. Balancing the
29 tendency for evolution to favour variants that increase the endemic load, we explore the impact of
30 vaccination strategies and non-pharmaceutical interventions (NPIs) that can counter these increases in
31 the impact of disease. We end with some open questions about the future of COVID-19 as an endemic
32 disease.

33 **Introduction**

34 Early in the global pandemic, COVID-19 levels rose and fell steeply, displaying rapid exponential
35 growth and leading to widespread lockdowns and other public health measures to slow transmission
36 (Ogden et al. 2022; Talic et al. 2021). The vaccination campaigns of 2021, followed by the nearly-
37 uncontrolled Omicron waves in early 2022 (Figure 1, BA.1 and BA.2 peaks), have now led to almost
38 100% immunological exposure in many countries. In Canada, for example, 100% of blood donors had
39 developed antibodies to the spike protein from previous exposure to the virus by June 2023, with 80%
40 also showing antibodies to nucleocapsid, indicating prior infection (Canadian Blood Services 2023). The
41 number of immunologically naïve individuals that fed COVID-19 dynamics throughout the pandemic
42 has now greatly decreased, but in its place is a continual flow of newly susceptible individuals as
43 humoral immunity wanes. For the past year, COVID-19 levels have ebbed and flowed in response to this
44 waning immunity, new variants, and to changing public health measures. These peaks and troughs are
45 more subdued wavelets, compared to earlier Omicron peaks (Figure 1).

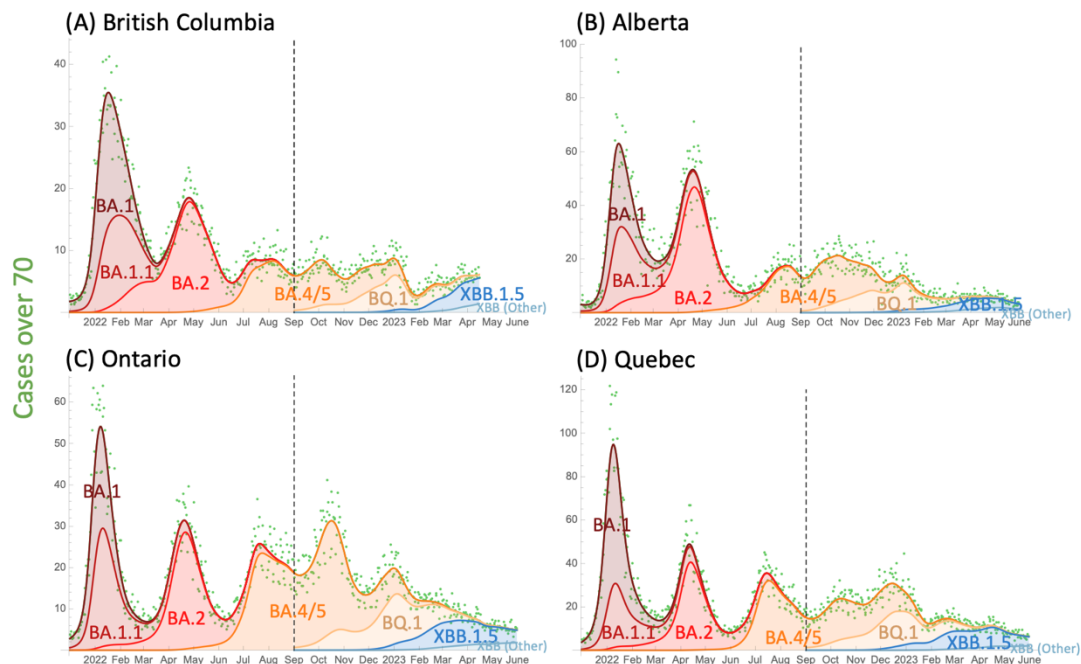


FIGURE 1: COVID-19 trends across four provinces in Canada. Major waves in early 2022 were driven by the rise and spread of Omicron, whose immune-evasive properties allowed widespread infection at a time when public health measures were largely relaxed (peak in January 2022: BA.1, April: BA.2, July: BA.4 & BA.5). A year later, Omicron variants have continued to spread rapidly (peak in December 2022: BQ.1; April 2023: XBB.1.5), but they no longer cause major waves in cases. PCR-confirmed cases per 100,000 individuals aged 70+ (green dots) are used to illustrate case trends, as testing practices changed dramatically over this time period but this age group remained eligible for testing. To guide the eye, a cubic spline fit ($\lambda=3$) was applied (top curves in each panel), and the frequency changes of each variant under this curve were fitted by maximum likelihood using duotang (CoVaRR-Net’s CAMEO 2023). Genomic sequence data from each province were obtained from the Canadian VirusSeq Portal (VirusSeq 2023) and fit by maximum likelihood to a model of selection in two periods: first 9 months using BA.1 as a reference (left of dashed line); second 9 months using BA.4/5 as a reference (right of dashed line), grouping all clades within a family together except when a sub-clade is also mentioned (e.g., BQ.1 separated from BA.5). See supplementary *Mathematica* file for scripts and duotang (CoVaRR-Net’s CAMEO 2023) for methodological details and finer resolution of lineages and time periods.

COVID-19 is now considered an endemic disease, being both widespread and persistent, adding to the respiratory infectious diseases with which we must routinely contend. Its now-endemic nature reflects a balance between waning immunity and on-going transmission, leading to a turnover of cases across the globe. Endemic does not mean “constant”, as new variants and behavioral shifts drive change. Endemic also does not mean “rare”, as waning and transmission rates have remained high (e.g., Figure 1). Here we explore mathematical models to improve understanding of how the ongoing evolution of SARS-CoV-2, as well as our behavioural responses, will shape endemic COVID-19 and similar diseases.

When most individuals in a population are susceptible (epidemic phase), any variant or behavioural measure that affects the transmission rate will have a direct effect on the number of new infections over the short term, as exposures determine the spread of disease. When a disease first appears, the reproductive number describing the number of new infections per infection, R_0 , is given by the transmission rate divided by the clearance rate of the infection in the classic SIR epidemiological model (Keeling and Rohani 2011). Thus, variants that increase transmission or behavioural changes that reduce transmission directly reduce new infections and the rate of exponential growth, but these new infections have little immediate effect on the large pool of susceptible individuals. Models of this epidemic phase (e.g., (Day et al. 2020)) also typically ignore waning of immunity or the possibility that variants may evade any such immunity earlier.

By contrast, when a disease is endemic and most individuals have some degree of immunity, waning must be explicitly considered and modeled in a manner that allows variants to infect earlier (as in the SIR_n model, with multiple recovered classes, that we consider here). Furthermore, any change in the transmission rate has a more complex effect on the number of infections in the near future, because higher transmissibility depletes the number of susceptible individuals whose immunity has waned (by “refreshing” that immunity through exposure), while lowering transmission allows susceptible individuals to accumulate.

Indeed, this kind of reasoning about endemic disease has been used as an argument against non-pharmaceutical measures like masking:

Masks “can delay transmission, they can reduce transmission, but they’re not actually effective measures at a population level,” because “exposure is essentially universal now to COVID-19.”

91 Public Health Officer, November 2, 2022 in [Today in BC podcast](#)

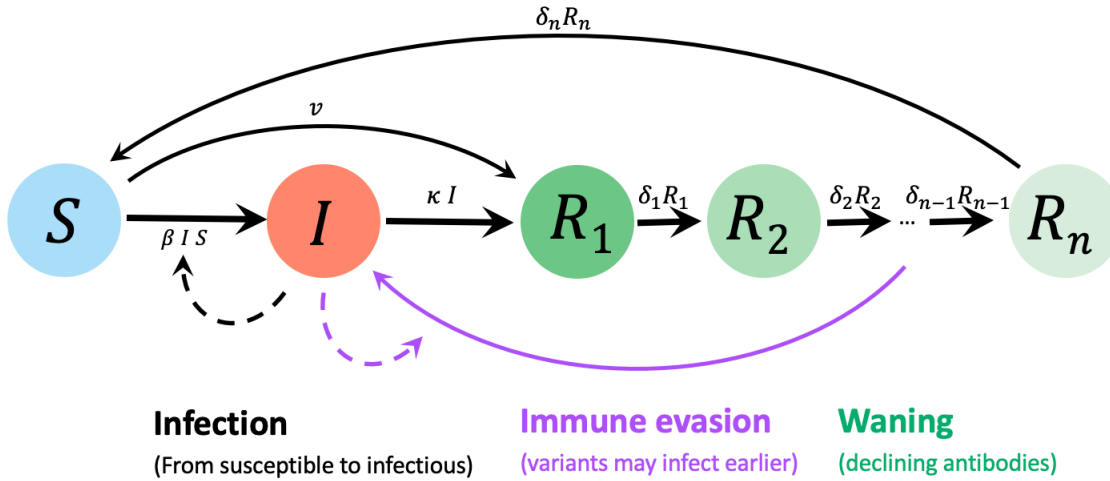
92 This argument assumes that transmission is so common that reducing risks of exposure no longer
93 matters, as another exposure will occur soon thereafter. This is a strong claim, with major implications
94 for both individual and public health decisions. It is essentially a claim that endemic levels of a disease
95 such as COVID-19 are not under our control.

96 Mathematical models can help evaluate such claims and determine whether and to what extent our
97 actions affect the endemic load of disease and mortality. Models can also predict how this load would
98 change in the face of new variants and how this depends on the properties of those variants. Here, we
99 tailor standard epidemiological models to the current phase of COVID-19 to better understand the risks
100 posed by new variants and our ability to control endemic diseases.

101

102 **Model background**

103 We use a classic compartment model, SIR_n , as illustrated in Figure 2, measuring the fraction of the
104 population that is in the susceptible class (S), the infectious class (I), or in one of several recovered
105 classes (R_j). These sequential recovered classes allow for different stages of waning immunity (i ,
106 ranging from 1 to n) and capture the dynamics of neutralizing antibodies that help protect against
107 infection (Andrews et al. 2022; Khoury et al. 2021). When measured on a log scale, neutralizing
108 antibodies rise to a high level soon after infection or vaccination and then decline linearly over time
109 since vaccination and/or infection (e.g., (E. H. Lau et al. 2021; Evans et al. 2022; C. S. Lau et al. 2022;
110 Jacobsen et al. 2023). We thus consider the R_j classes to fall along different stages of this linear decline
111 (R_1 being highest and R_n lowest), with antibody levels falling over time (modeled as movement of
112 individuals from R_j to R_{j+1}) until levels are so low that infection is no longer prevented (R_n waning to S).



113

114 **FIGURE 2: Epidemiological model used to predict impact of changing variants, behaviour,**
 115 **and policy on endemic levels of disease.** We consider populations that have a high level of
 116 immunity due to prior infection and/or vaccination and that consist of S : a susceptible fraction, I :
 117 an infected fraction, and R_j : a recovered fraction with immunity at different stages of waning.
 118 Parameters are β : transmission rate, κ : recovery rate, δ_j : per-class waning rate per day, and v :
 119 vaccination rate at the population level, all measured in the present-day population with prior
 120 exposure. Movement between adjacent recovered classes is set equal to $\delta_j = n\delta$, so that the
 121 expected time between first recovering and returning to the susceptible state is $1/\delta$ days.

122 As we are modelling the long-term epidemiological dynamics in a population previously exposed to the
 123 virus via vaccinations and/or infections, we emphasize that the susceptible class, S , consists of
 124 individuals who have had previous exposure but are currently susceptible due to waning immunity.
 125 Throughout this paper, we are thus describing the epidemiological dynamics in a previously challenged
 126 population.

127 When we model vaccination, vaccines move individuals from the susceptible (S) to the first recovered
 128 class (R_1) at rate v per population (Figure 2). We consider v to be the total fraction of the population
 129 moved (rather than the rate per susceptible individual) to align with data on observed or target
 130 vaccination rates within a country. Vaccination is therefore protective against infection in this model
 131 until vaccine-induced immunity wanes, which occurs at the same rate that infection-induced immunity
 132 wanes (although we do extend the model to consider the possibility that vaccination does not elicit an
 133 immune reaction in some individuals). We do not separately model disease or severity, or vaccine's
 134 effectiveness against these as distinct from protection against infection.

135 Before considering variants or NPI measures, the dynamics describing changes in the number of
 136 individuals in each compartment within the SIR_n model are:

137
$$\frac{dS}{dt} = \delta_n R_n - \beta SI - v$$

138
$$\frac{dI}{dt} = \beta SI - \kappa I \tag{1}$$

139
$$\frac{dR_1}{dt} = \kappa I + v - \delta_1 R_1$$

140
$$\frac{dR_j}{dt} = \delta_{j-1} R_{j-1} - \delta_j R_j \quad \text{for } 2 \leq j \leq n.$$

141 We can find the equilibria of this system of equations by setting the derivatives to zero and solving,
 142 yielding two equilibria for the fraction of individuals in each class. One equilibrium corresponds to the
 143 disease being absent ($\hat{S} = 1$), and the other to the disease being endemic:

144
$$\hat{S} = \frac{\kappa}{\beta}$$

145
$$\hat{I} = \left(1 - \frac{\kappa}{\beta}\right) \frac{\delta}{\delta + \kappa} - \frac{v}{\delta + \kappa} \quad (2)$$

146
$$\hat{R}_j = \frac{1}{n} \left(\left(1 - \frac{\kappa}{\beta}\right) \frac{\kappa}{\delta + \kappa} + \frac{v}{\delta + \kappa} \right) \quad \text{for } 1 \leq j \leq n.$$

147 Importantly, because we are explicitly modelling endemic COVID-19 most individuals have previously
 148 been exposed to SARS-CoV-2, susceptibility and infectiousness may be lower in the current population
 149 than when the virus first appeared in humans because of cellular immunity, any residual humoral
 150 immunity among susceptible individuals (Tan et al. 2023), and/or due to any behavioural changes
 151 (including better ventilation, testing and self-isolation practices). For example, the rapid induction of
 152 cellular immunity reduces the viral load of typical breakthrough infections (Puhach et al. 2022),
 153 lowering transmission (β) compared to a fully naïve population. The epidemiological dynamics in this
 154 endemic model thus depend on an "*endemic basic reproductive number*", $\tilde{R}_0 \equiv \beta/\kappa$, which is the basic
 155 reproductive number in a population consisting entirely of currently susceptible, but previously
 156 vaccinated or infected, individuals whose immunity has waned. In contrast to the initial R_0 for COVID-
 157 19 at the time of its emergence, the parameters of the endemic model and in \tilde{R}_0 (transmission, β , and
 158 recovery, κ) refer to rates in this previously challenged population. Our estimates of \tilde{R}_0 range from 1 to
 159 6 (Appendix 1), depending on estimates used for recovery rates, waning, and the endemic level of
 160 infections within a population, with a value of $\tilde{R}_0 \approx 2$ for the parameters considered typical (Table S1).

161 If this previously challenged population were fully susceptible (\hat{S} near one), the disease would spread
 162 when rare as long as transmission rates were higher than recovery rates, $\tilde{R}_0 = \frac{\beta}{\kappa} > 1$, which we assume
 163 to hold. In this case, the endemic equilibrium (2) exists and is stable for all examples considered here.
 164 The endemic equilibrium may, however, be unstable (Hethcote, Stech, and Van Den Driessche 1981),
 165 leading to sustained cyclic dynamics, outside of the parameters used here (e.g., for n large enough).

166 The equilibrium can also be written in terms of \tilde{R}_0 as:

167
$$\hat{S} = \frac{1}{\tilde{R}_0}$$

168
$$\hat{I} = \left(1 - \frac{1}{\tilde{R}_0}\right) \frac{\delta}{\delta + \kappa} - \frac{v}{\delta + \kappa} \quad (3)$$

169
$$\hat{R}_j = \frac{1}{n} \left(\left(1 - \frac{1}{\hat{R}_0} \right) \frac{\kappa}{\delta + \kappa} + \frac{v}{\delta + \kappa} \right) \quad \text{for } 1 \leq j \leq n.$$

170 Also of relevance is the number of bouts of disease that an individual expects per year, which is
 171 $365 \beta \hat{S} \hat{I} = 365 \kappa \hat{I}$, assuming average behaviour (see Table S1).

172 Given that recovery rates are higher than waning rates ($\delta \ll \kappa$), equation (3) shows that the number of
 173 infectious individuals at the endemic equilibrium is reduced by the number of vaccinations within a
 174 typical recovery period (v/κ). If more vaccinations were to be given in a typical recovery period than
 175 the fraction of individuals expected to be infectious in the absence of vaccination, the disease could be
 176 driven extinct locally (though we note that in this model vaccination has a very high, if temporary,
 177 efficacy against infection, and that reintroductions are expected from importations, animal reservoirs,
 178 and chronic infections). Uptake of additional vaccine doses during 2023 has, however, been so low in
 179 many countries as to make little difference to the incidence and dynamics of SARS-CoV-2 (e.g., daily
 180 [annual] rates of 0.012% [4.7%] in France and 0.023% [8.8%] in the United States from 1 January – 30
 181 April, 2023; (Our World in Data 2023)). To simplify the discussion, we ignore ongoing vaccination for
 182 now, returning later to a discussion of the impact that vaccination uptake can have on individual risks of
 183 infection and on the overall incidence of disease.

184 **Spread of variants during the endemic phase**

185 A new variant may spread within the population if it is more transmissible (e.g., better binding to ACE2
 186 receptors on host cells), more immune evasive, or both (see (Cao et al. 2023) for empirical measures for
 187 SARS-CoV-2). We can calculate the rate of spread of a variant using the SIR_n model by allowing
 188 different transmission rates for the resident variant (β) and the new variant ($\beta^* = \beta + \Delta\beta$) and by
 189 allowing immune evasive variants to infect earlier than the resident strain, while antibody levels are at
 190 intermediate levels. Specifically, we assume that an immune evasive variant can infect the last m
 191 recovered classes (each of which is at frequency \hat{R}_j at the endemic equilibrium given by (3)), as well as
 192 susceptible individuals.

193 As described in Appendix 1, a new variant introduced into a population at the endemic equilibrium has a
 194 selective advantage of:

195
$$s = \underbrace{\frac{\Delta\beta}{\beta} \kappa}_{\text{Transmission advantage}} + \underbrace{m \hat{R}_n \beta^*}_{\text{Evasion advantage}} \quad (4)$$

196 The selection coefficient, s , describes the rate at which the new variant spreads relative to the resident
 197 variant. Selection coefficients describing evolutionary changes in SARS-CoV-2 have been estimated in
 198 many jurisdictions using sequence information and are often relatively stable over time and space when
 199 measured consistently against the same reference strain (van Dorp et al. 2021; Otto et al. 2021).

200 What are the consequences of spreading variants for the incidence of disease? The incidence is initially
 201 expected to rise exponentially at rate proportional to selection (specifically, $s \hat{I}$), but this is only transient
 202 as the new variant spreads through the susceptible population available to it. Over the long term, we
 203 show that the impact on the endemic level of disease depends strongly on whether the variant increases
 204 transmission rates and/or increases immune evasiveness, as well as the persistence of immune evasion
 205 during subsequent infections, even for variants with the same selective advantage.

206 In particular, when the population is comprised entirely of the new variant, the endemic level of disease
207 changes to:

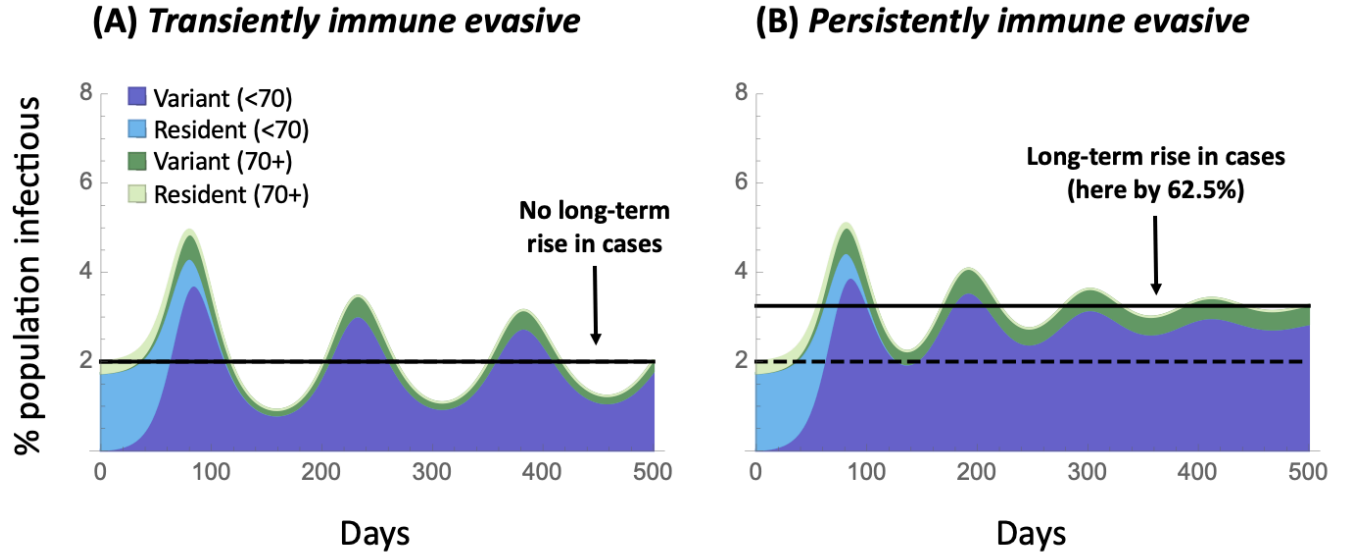
$$208 \quad \hat{I}^* = \left(1 - \frac{\kappa}{\beta + \Delta\beta}\right) \frac{\delta + \Delta\delta}{\delta + \Delta\delta + \kappa} \quad (5)$$

209 (found by solving equation (A1) for the endemic equilibrium when only the variant is present). The term
210 $\Delta\delta$ refers to how the variant changes the rate of complete waning, from first entering the recovered class
211 to returning to the susceptible state (i.e., $1/(\delta + \Delta\delta)$ is the mean number of days to return to
212 susceptibility). [As short-hand, we refer to a variant's impact on immune evasion as a change in the
213 waning rate $\Delta\delta$, but the model actually assumes log-antibody levels wane at a constant rate but the
214 variants can just infect earlier, becoming susceptible sooner.]

215 Equation (5) allows us to evaluate the long-term impact of different types of variants. For immune
216 evasive variants, the results are strongly dependent on the variant-specific immunity that develops after
217 infection, even if the lineages have the same selective advantage and rate of spread (s , equation (4)).
218 Consider two extreme possibilities:

- 219 • **Transient immune evasiveness:** If the variant better evades the initial suite of antibodies but
220 causes infections that generate variant-specific immunity, subsequent infections may no longer
221 be immune evasive. In this case, subsequent infections would require the full waning period
222 (returning to the S compartment and not the R_i compartments), as for the resident strain. With
223 only transient evasiveness, the long-term level of COVID-19 is *unaffected* ($\Delta\delta = 0$).
- 224 • **Persistent immune evasiveness:** If the variant allows infections to occur earlier, both in the first
225 and in subsequent infections, then the rate of return to susceptibility is consistently higher ($\Delta\delta =$
226 $\frac{m}{n-m}\delta$). With waning slow relative to recovery ($\delta + \Delta\delta \ll \kappa$), persistently immune evasive
227 variants cause the incidence of disease to *rise in proportion* to the increased rate of waning, $\hat{I}^* \approx$
228 $\hat{I} (1 + \Delta\delta/\delta)$.

229 In either case, immune-evasive variants spread in the short-term because of the selective advantage, s ,
230 gained by infecting susceptible individuals earlier, but the subsequent dynamics and long-term impact
231 differ greatly, depending on whether variant-specific immunity builds (Figure 3). The extent to which
232 exposure to a variant elicits variant-specific humoral or cellular immunity almost certainly falls between
233 these two extremes. Metanalyses suggest, for example, that infections with Omicron are less protective
234 against reinfection with Omicron, compared to the protective effects of pre-Omicron variants,
235 suggesting some persistence in its immune-evasive properties (Arabi et al. 2023).



236 **FIGURE 3: Impact of the spread of immune evasive variants depends on whether a variant-**
 237 **specific immune response is elicited.** Plots illustrate the dynamics over time of a more immune
 238 evasive variant, which is able to infect earlier in the waning period (by $m = 2$ out of $n = 5$
 239 recovered classes), giving the variant an $s = 8.3\%$ selective advantage per day, which lies in the
 240 range of the faster spreading variants observed in the past year (CoVaRR-Net’s CAMEO 2023).
 241 While the short-term spread of the variant (dark shading taking over from light shading) and rise in
 242 cases are nearly identical (given s is the same), the long-term consequences differ substantially
 243 depending on whether the variant’s evasive properties are (panel A) transient or (panel B)
 244 persistent. The endemic equilibrium rises only if evasiveness persists in subsequent infections
 245 (panel B). We illustrate the dynamics in younger (under 70) and older (70+) individuals, who are
 246 more prone to severe cases. Parameters: $\kappa = 0.2$, $\delta = 0.008$, $\hat{I} = 2\%$, $\beta = 0.42$, the nominal
 247 parameter estimates given in Appendix 1 for all age classes.

248 By contrast, more transmissible variants change the endemic equilibrium to:

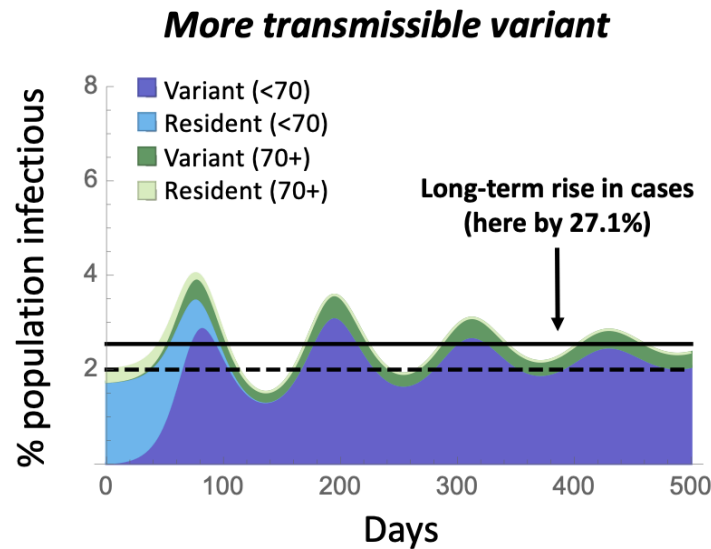
$$249 \quad \hat{I}^* = \hat{I} \left(1 + \frac{1}{\tilde{R}_0 - 1} \frac{\Delta\beta}{\beta + \Delta\beta} \right). \quad (6)$$

250 As a consequence:

- 251 • **More transmissible variants:** If the variant increases transmission rate, spread in the short term
 252 depends directly on the change in transmission ($s = (\Delta\beta/\beta) \kappa$; equation (4)), while the long-
 253 term impact on the incidence of disease exhibits diminishing returns (\hat{I}^*/\hat{I} depends on
 254 $\Delta\beta/(\beta + \Delta\beta)$). Thus, more transmissible variants have **a less than proportionate influence** on
 255 the number of cases in the long term, unless the susceptible pool is large and \tilde{R}_0 small ($\hat{S} =$
 256 $1/\tilde{R}_0 > 1/2$).

257 While more immune evasive variants increase the pool of susceptible individuals available to them (in
 258 our model, by adding the last m recovered classes to the susceptible class), more transmissible variants
 259 deplete the susceptible pool. This can be seen by the effect on the susceptible class at equilibrium, which
 260 decreases from $\hat{S} = \kappa/\beta$ for the resident virus to $\hat{S}^* = \kappa/(\beta + \Delta\beta)$ for a more transmissible virus. For
 261 this reason, more transmissible viruses are, to some extent, self-limiting and often have less of an effect
 262 on the long-term number of cases than seen for a permanently immune evasive variant. Thus is
 263 illustrated in Figure 4, which shows that the equilibrium rises less for a given % increase in

264 transmissibility (panel C) than for the same % increase in waning rate for a permanently immune
 265 evasive variant (panel B), unless \tilde{R}_0 is so small that most individuals in the population are susceptible.
 266 Of course, variants may combine features affecting transmissibility and immune evasiveness (Cao et al.
 267 2023), as explored in Figure S1.



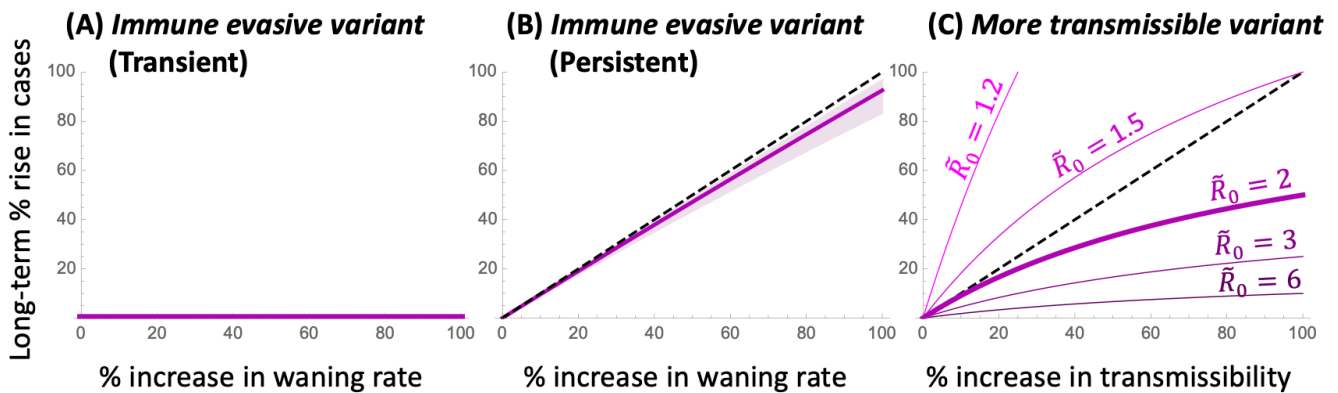
268 **FIGURE 4: Impact of the spread of a more transmissible variant.** Plot illustrates the dynamics
 269 over time of a more transmissible variant, which increases β (and hence \tilde{R}_0) by 42%, chosen to
 270 give the variant the same selective advantage as in Figure 3 ($s = 8.3\%$). While exhibiting a similar
 271 short-term rise in cases as in Figure 3, the long-term impact is intermediate. Parameters are
 272 identical to Figure 3, with $\beta^* = 0.59$.

273 This model predicts, as seen in the data over the past year (Figure 1), only modest rises and falls in case
 274 numbers, despite substantial evolutionary change in the frequency of different variants. This occurs
 275 because of the substantial population-level immunity that persists in the population at the endemic
 276 equilibrium. With a mixture of susceptible, infectious, and recovered individuals, the effective
 277 reproductive number at the endemic equilibrium must be one ($R_{e,t} = 1$) for the resident and $R_{e,t} = 1 +$
 278 $\Delta\beta/\beta$ for a more transmissible variant (e.g., $R_{e,t} = 1.42$ in Figure 4). Thus, only a modest drop in the
 279 susceptible population is needed ($1/R_{e,t}$) before the infectious class peaks and falls again.

280 The robustness of these conclusions is explored in Appendix 2, considering different models of
 281 immunity (including leaky immunity) and the inclusion of features such as an exposed class and failure
 282 to seroconvert. The strength of selection (equation (4)) and the long-term impact on endemic levels of
 283 disease (equation (5)) are robustly observed. The speed at which the waves dissipate over time, however,
 284 is sensitive to model assumptions, stabilizing faster than observed above in many cases (Figure S2), so
 285 we caution that the nature of subsequent wavelets caused by the spread of a variant is hard to predict.

286 We conclude that variants may have dramatically different long-term impacts on the level of disease
 287 depending on the nature of the advantage (transiently or persistently immune evasive and/or more
 288 transmissible), despite exhibiting the same selective advantage and hence spreading at the same rate
 289 (e.g., with selection of $s = 8.3\%$ per day in Figures 3 and 4). Indeed, a variant that is transiently immune
 290 evasive but less transmissible can spread and would be expected to reduce the equilibrium level of
 291 disease, except that once immunity to this variant has built, the previous resident reemerges because of
 292 its higher transmissibility (Figure S1B).

293 Figure 5 shows these long-term impacts on disease incidence at the endemic equilibrium across the
 294 range of plausible parameters (Appendix 1). Transiently immune evasive variants have no long-term
 295 impact (panel A), whereas the rise in cases is nearly proportional to the ability of a variant to evade
 296 immunity, if that evasiveness is persistent, regardless of the exact parameter values (panel B). By
 297 contrast, the long-term impact of a more transmissible variant depends strongly on the current
 298 transmissibility, as measured by the endemic reproductive number. The larger \tilde{R}_0 is, the smaller the
 299 long-term impact of more transmissible variants is on disease levels (Figure 5C), essentially because the
 300 pool of susceptible individuals is then smaller and rapidly depleted by more transmissible variants ($\hat{S} =$
 301 $1/\tilde{R}_0$). That said, for given waning (δ) and recovery (κ) rates, the endemic level of disease is higher
 302 when \tilde{R}_0 is higher (equation (3)), so a small percentage increase in disease incidence can still have a
 303 numerically important impact on the burden of disease.



304

305 **FIGURE 5: Long-term impact of a variant.** The percent change in the endemic equilibrium is
 306 shown as a function of the percent by which the variant increases the rate at which recovered
 307 individuals become susceptible again ($\Delta\delta$, panels A,B) or transmissibility ($\Delta\beta$, panel C).
 308 Transiently immune evasive variants have no long-term impact, while persistently immune evasive
 309 variants cause the endemic incidence of disease to rise nearly in proportion (dashed curve) across
 310 all parameters considered plausible (purple shading, with the nominal parameter values illustrated
 311 by a thick purple curve; see Appendix 1 and Table S1). By contrast, the impact of a more
 312 transmissible variant that increases β depends strongly on \tilde{R}_0 (but none of the other parameters),
 313 leading to a less than proportional rise in cases whenever $\tilde{R}_0 \geq 2$ (see equation (6)).

314 **Controlling an endemic disease** – In the face of variants that are increasingly transmissible and/or
 315 persistently immune evasive, the endemic level of disease is expected to rise over time, but these
 316 increases can be countered by protective measures at the individual and population level. Protective
 317 measures range from vaccination to NPI measures, such as testing and self-isolation, avoiding crowded
 318 indoor spaces, improving ventilation, and the wearing of well-fitting and high-quality masks (The Royal
 319 Society 2023). Here we explore the impact of these protective measures at both the individual level,
 320 modulating the frequency of infections, and the population level, modulating the endemic incidence of
 321 disease.

322 **Vaccination** – Vaccination allows individuals to short-circuit the disease cycle by boosting antibody
 323 levels and immunity by another dose rather than by infection. Globally, 65% of people have had the
 324 primary series of COVID-19 vaccines but an average of only 0.35 booster doses have been distributed
 325 per person ((Our World in Data 2023); accessed 22 August 2023). Jurisdictions vary widely in
 326 recommended vaccine schedules and access to vaccines. For example, only individuals at higher risk of

327 serious illness are eligible for COVID-19 vaccinations in the United Kingdom (NHS 2023). In Canada,
328 the National Advisory Committee on Immunization recommends that all adults be offered vaccines six
329 months after the last dose or infection (NACI 2023). The Centre for Disease Control in the USA,
330 however, recommends that individuals stay up to date with important vaccine updates (e.g., the updated
331 mRNA vaccines providing protection against BA.4 and BA.5 in the fall of 2022 and against XBB in the
332 fall of 2023 (CDC 2023)).

333 There is substantial uncertainty and confusion in both public and public health circles about the value of
334 regular vaccinations against COVID-19 (Lin et al. 2023). Here, we explore one aspect: how much do
335 regular vaccinations reduce the burden of disease expected at an endemic equilibrium?

336 We consider the impact of policies aimed at future vaccine uptake, encouraging vaccination of a portion
337 of the population (v) per day. Given that vaccines are recommended only after a substantial amount of time
338 has passed since the previous dose or infection, these vaccinees are assumed to target individuals in the
339 susceptible class, moving them into the first recovered class (S to R_1 ; equation (1)). Unlike many
340 previous epidemiological models (reviewed in (Scherer and McLean 2002)), we assume that the target
341 vaccination rate is set by policy, adjusting public health campaigns, vaccine cost, and availability to
342 meet these targets (i.e., dS/dt in equation (1) declines by a fixed daily rate, v , rather than a per capita
343 rate, vS).

344 We consider vaccination rates in Canada as typical of what can be achieved when vaccines are available
345 at regular intervals (every six months). From April-July 2023, vaccination rates in Canada have
346 averaged only 0.012% of the population per day (annual rate of 4.5% (Health Infobase Canada 2023)).
347 While these vaccinations help those individuals receiving a dose, this level has a negligible impact on
348 the endemic level of cases (decreasing \hat{I} from 2% to 1.94% for the nominal parameter values). Many
349 public health agencies have encouraged COVID-19 vaccine updates in the fall (Mahase 2023). For
350 example, vaccination rates in Canada during September-December 2022 were 14 times higher (0.174%
351 of the population per day, an annual rate of 63.5% (Health Infobase Canada 2023)), a rate that
352 substantially lowers the endemic equilibrium level if maintained (from 2% to 1.16% for the nominal
353 parameter values).

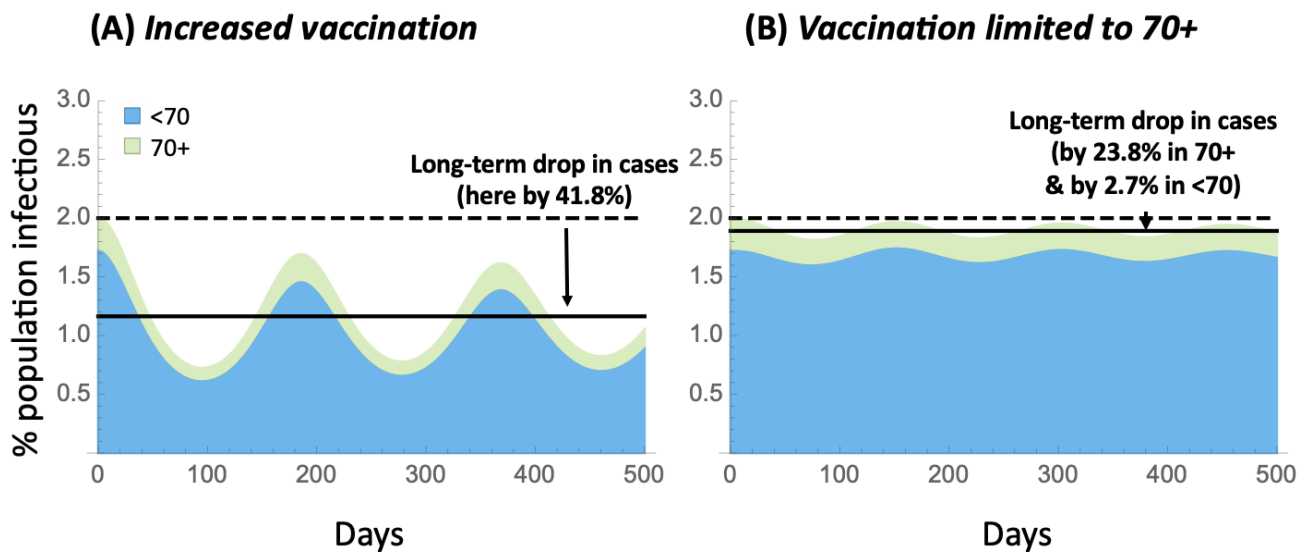
354 At an individual level, vaccination reduces the number of infections that one expects to have.
355 Individuals on a regular six-month vaccination schedule are expected to be protected from neutralizing
356 antibodies for $1/\delta$ out of every 180 days. Calculating the probability of waning and infection before
357 their next vaccine (equation (A2); Appendix 1), a regularly vaccinated individual expects to have about
358 60% as many infections per year (0.88 vs 1.46) for the nominal parameter values (Appendix 1). Across
359 the range of parameters considered plausible, vaccination every six months leads to only 40%-66% as
360 many infections annually (supplementary *Mathematica* file).

361 At a population level, in our model, vaccination reduces the endemic level of infections to $\hat{I}_v = \hat{I} - \frac{v}{\delta + \kappa}$
362 (equation (2)). That is, the endemic level of infections is reduced by approximately the number of
363 vaccinations conducted during the infectious period (v/κ , given that waning is considerably slower than
364 recovery). Figure 6 illustrates the impact of increasing and maintaining the vaccination rate at the higher
365 levels observed in Canada in the fall of 2022 ($v = 0.174\%$). In this case, the long-term incidence of
366 infection can be driven down by $\sim 42\%$ (panel A). Across the range of parameters considered in
367 Appendix 1, this population-level benefit ranging from a 12-100% decline in incidence of disease,
368 falling at the lower end of the benefit when disease incidence is high without vaccination ($\hat{I} = 4\%$) but

369 at the higher end and allowing complete eradication when disease incidence is low without vaccination
370 ($\hat{I} = 0.5\%$).

371 One policy option considered in many jurisdictions is to regularly vaccinate only the more vulnerable
372 segment of the population. Figure 6B illustrates, however, that limiting vaccination to the more
373 vulnerable population (shown here as vaccinating only those over 70 at a rate $v = 0.174\%$) has less
374 impact on the frequency of infections experienced by this vulnerable population (reduced by only 24%),
375 because the incidence of COVID-19 remains high overall, increasing their risk of exposure.

376 That said, the additional protection provided by COVID-19 vaccines against severe disease, above and
377 beyond the protection provided against infection, means that the risk of hospitalization and death can be
378 lowered by vaccinating the vulnerable (Nyberg et al. 2022; Chemaitelly et al. 2022). Further reducing
379 the risk of infection and severe disease, however, requires a broader vaccination campaign. Broad
380 vaccination campaigns provide additional protection for the vulnerable, while also reducing the number
381 of sick days, risks of long COVID, and severe disease among those not known to be vulnerable.



382

383 **FIGURE 6: Impact of vaccination strategies.** Plots illustrate the dynamics over time when
384 vaccination is increased to 0.174% of the population per day (annual rate of 63.5%), either (A)
385 within the entire population or (B) limited to a more vulnerable population (illustrated as 70+ in
386 age). Parameters are identical to Figure 3, with $v = 0.00174$.

387 As noted in Appendix 2, seroconversion rates upon vaccination are high (Wei et al. 2021), so we do not
388 correct v for the small fraction of doses that fail to elicit an immune response. Not all individuals will,
389 however, achieve high levels of immunity following vaccination and not all will be protected from
390 infection. A mixture of induced immunity could be modelled by moving vaccinated individuals into a
391 distribution of R_j classes. Additionally, some individuals being vaccinated may have been exposed in
392 the recent past (i.e., coming from the infectious or recovered compartments, not solely from the
393 susceptible classes). These possibilities are not explicitly modeled, although they would lower the
394 protection offered by vaccination, akin to lowering v , and so require higher vaccination uptake to
395 achieve the benefits described above.

396 *NPI measures* – A wide variety of non-pharmaceutical interventions have been deployed to counter the
397 spread of SARS-CoV-2, including testing and self-isolation, enhancing ventilation and air filtration, and

398 wearing of high quality masks (see evaluation of evidence in the report (The Royal Society 2023)).
 399 Here, we consider the individual-level and population-level benefits of NPIs, as a function of their
 400 impact on preventing transmission of the virus, modelled by NPIs preventing a portion p of
 401 transmissions both from and to NPI users. Specifically, we assume that the NPI measures reduce
 402 transmission from β to $(1 - p)\beta$ if one member in an interaction practices the measures and to
 403 $(1 - p)^2\beta$ if both do. The population is assumed to be heterogenous, as illustrated in Figure S4,
 404 consisting of a fraction f who regularly engage in NPI measures and are denoted by a \ddagger (compartments
 405 $S^\ddagger, I^\ddagger, R_j^\ddagger$ for $j = 1$ to n , which sum to f) and a fraction $1 - f$ who do not (compartments S, I, R_j , which
 406 sum to $1 - f$). See Appendix 3 for model details.

407 We first determine the benefit to an individual who adheres to NPI measures (e.g., masking). At the
 408 endemic equilibrium, an individual engaging in the NPI measure has a lower risk of being infected at
 409 any given point in time of:

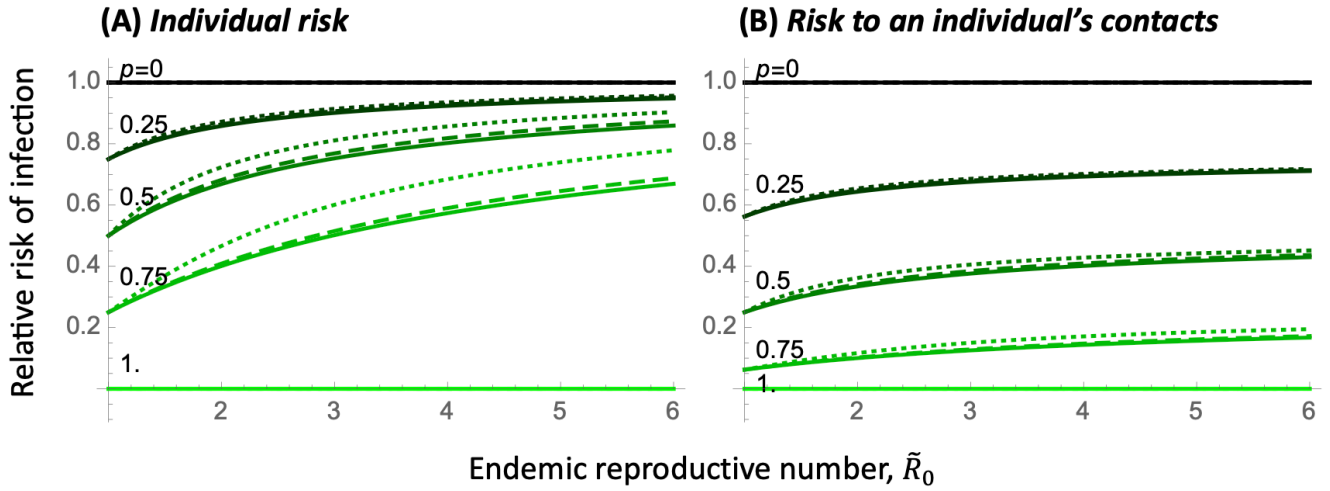
410 Relative risk of infection:
$$\frac{\hat{i}^\ddagger / f}{\hat{i} / (1-f)} = \frac{1}{1 + \hat{S} \frac{p}{(1-p)(1-f)}}, \quad (7)$$

411 where \hat{S} is the fraction of the population at the endemic equilibrium who are susceptible and do not
 412 engage in the NPI measure (given by (A11), $\hat{S} \approx \kappa/\beta$ when f is small). This relative risk is
 413 mathematically equivalent to the relative rate at which individuals become infected for those who do
 414 versus do not engage in the NPI measure, as well as the relative number of infections expected per year.

415 Figure 7 illustrates the relative risk of infection (equation (7)). As expected, the more effective the NPI
 416 measure is (the higher p) the lower the relative risk to individuals who engage in the NPIs (panel A).
 417 This individual-level benefit is only weakly dependent on the fraction of the population currently
 418 engaging in these measures ($f = 10\%$, 50% , and 90% shown as solid, dashed, and dotted curves), with
 419 the relative risk rising slightly as f increases because non-practitioners gain a slight benefit from those
 420 who do practice the NPI measure.

421 The individual benefits depend strongly, however, on the endemic reproductive number of the disease
 422 (\tilde{R}_0). At the nominal value of $\tilde{R}_0 = 2$ and assuming low population-level uptake (f small), a person's
 423 relative risk of infection can be substantially reduced for NPIs that provide fairly modest protection (by
 424 14% and by 33% for $p = 25\%$ and 50% , respectively). For $\tilde{R}_0 = 6$ (on the high end of the range
 425 considered plausible; Appendix 1), however, these individual-level benefits diminish (to 5% and 14%
 426 for $p = 25\%$ and 50% , respectively), because individuals are exposed so often that modestly protective
 427 NPIs only moderately delay infection.

428 Not only is a susceptible individual who regularly engages in NPI measures less likely to become
 429 infected when in contact with an infectious individual (by a factor $1 - p$), but they are also less likely to
 430 pass the infection on to one of their contacts (by another factor $1 - p$), compared to a non-practicing
 431 individual who is currently susceptible. Accounting for the proportion of time that practicing and non-
 432 practicing individuals are susceptible (as in equation (7)), the risk per unit time of being infectious and
 433 infecting a contact is substantially lowered for those engaging in NPI measures relative to those who do
 434 not (Figure 7B). This validates the approach used by many who adhere to NPI measures, such as
 435 masking, in order to protect vulnerable relatives and close contacts.



436

437

438

439

440

441

442

443

444

FIGURE 7: Risk of infection for individuals regularly engaging in an NPI measure such as masking, relative to unmasked individuals. Coloured lines illustrate different levels of protection, p , provided by the NPI measure, in a population where the fraction of individuals engaging in the NPI measure is $f=10\%$ (solid), 50% (dashed), and 90% (dotted). Panel A shows the risk of infection and panel B the risk of becoming infected and infecting a contact for an individual engaging in NPI measures, relative to those who do not. The x-axis gives the endemic reproductive number in this heterogeneous population, $\tilde{R}_0 = ((1-f) + f(1-p)^2) \beta / \kappa$. Parameters: Relative risk depends on the parameters only through \tilde{R}_0, f , and p .

445

446

447

The curvature of the relative risks in Figure 7 highlights the utility of multiple complementary interventions: other policies that reduce transmission (lowering \tilde{R}_0) make masking more effective to individuals, because those individuals are less repeatedly exposed.

448

449

450

451

452

453

454

455

456

The individual-level benefits of NPI measures diminish with \tilde{R}_0 (x-axis of Figure 7) because individuals practicing NPI measures are more likely than non-practitioners to have remained uninfected and so are more often susceptible at the time of exposure, which increases their relative risk of infection as \tilde{R}_0 increases. Different results are obtained if individuals frequently switch their behaviour (e.g., masking some days and not others). Modifying the model as described by equation (A12), all individuals are then equally likely to be susceptible on any given day, and the NPI measure always reduces the risk of infection by a factor $(1-p)$ for each practicing individual in an interaction. That is, the benefits remain at their maximal value of $(1-p)$ in panel A and $(1-p)^2$ in panel B, regardless of \tilde{R}_0 and f (Appendix 3).

457

458

459

We next evaluate the population-level advantages of NPI measures by calculating the fraction of infected individuals expected at the endemic equilibrium ($\hat{I} + \hat{I}^\ddagger$) when a fraction f of the population upholds these measures, relative to a population in which nobody does:

460

$$\text{Relative fraction of population infected: } \frac{\hat{I} + \hat{I}^\ddagger}{(\hat{I} + \hat{I}^\ddagger)_{f=0}} = (1 - \hat{S} - \hat{S}^\ddagger) \frac{\tilde{R}_0}{\tilde{R}_0 - 1}, \quad (8)$$

461

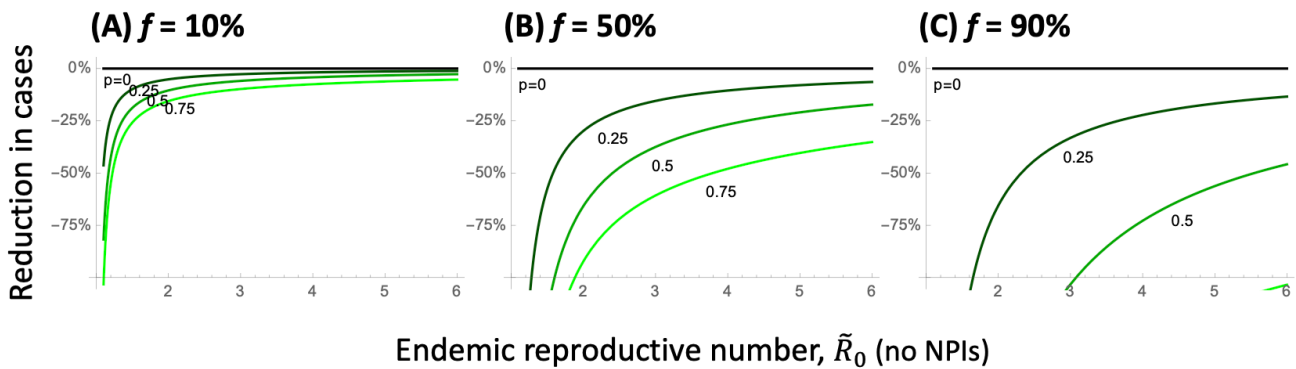
462

463

using the equilibrium values given by equation (A11). The right-hand side of equation (8) emphasizes that the population-wide benefits increase (fewer people will be infected) when there are more susceptible individuals available ($\hat{S} + \hat{S}^\ddagger$ larger).

464 While the population-level impact is small when few individuals mask (left panel of Figure 8), there are
 465 substantial benefits to having moderate to high adherence to the NPI measures (central and right panel).
 466 These benefits are strongest when the endemic reproductive number is small, potentially moving the
 467 population away from the endemic case, where COVID-19 persists, to the disease-free equilibrium
 468 (when the curves cross the x-axis), again emphasizing the added benefits that come from combining
 469 interventions.

470 The reduction in cases caused by NPI measures is expected to result in a proportionate reduction in
 471 severe cases and deaths. Even a modest reduction (say 20%) can have non-linear benefits when
 472 hospitals are at capacity, improving care for all (Wichmann and Wichmann 2023). Achieving such
 473 benefits at a population level, however, requires that there be clear messaging and incentives to obtain
 474 the moderate to high levels of uptake required to impact population-wide infection rates.



475

476 **FIGURE 8: Reduction in cases at the endemic equilibrium when a fraction f of the**
 477 **population engages in an NPI measure, relative to when none do.** Coloured curves illustrate
 478 different levels of protection, p , provided by the NPI measure. Panels show the fraction of the
 479 population practicing the NPI measure: (A) $f = 10\%$, (B) 50% , and (C) 90% . The x-axis gives the
 480 endemic reproductive number in a population that is not engaging in the NPI measure, given by
 481 $\tilde{R}_0 = \beta/\kappa$. Parameters: Reduction in cases depends on the parameters only through \tilde{R}_0, f , and p .

482 **Discussion –**

483 This paper aims to expand our understanding of the impact of variants, as well as behavioural and public
 484 health measures, on endemic diseases like COVID-19. Widespread measures, both by individuals and
 485 public health agencies, repeatedly “flattened the curve” of COVID-19 during the first two years of the
 486 pandemic, reducing viral transmission to save lives and avoid collapse of health care systems (Ogden et
 487 al. 2022; Talic et al. 2021). Since mid-2022, however, COVID-19 has persisted at high levels throughout
 488 the world, becoming endemic with no sign of abating even during summer months. The mantra to
 489 “flatten the curve” is no longer relevant, as endemic levels are already fairly flat, and we lack a
 490 compelling guide to govern our collective behaviour in its place.

491 For COVID-19, endemic does not mean constant, with wavelets caused by variants, changing behaviour,
 492 and varying vaccination rates. Nor does endemic mean rare, as on-going high levels of COVID-19
 493 health impacts remain. Nor does endemic mean out of our control, as protective measures continue to
 494 have important benefits, boosting immunity through vaccination and reducing transmission through
 495 effective NPI measures. The goal of this paper is two-fold: to explore the impact of evolutionary

496 changes in the virus on disease incidence and to discuss how protective measures can counteract these
497 rises, reducing disease risks.

498 Variants of endemic diseases that increase transmissibility and/or immune evasion are selectively
499 favoured, with rises in frequency that can be measured empirically, yielding estimates of the strength of
500 selection (s). While the strength of selection accurately predicts the speed with which one variant
501 replaces another, it does not predict the long-term impact on endemic levels of disease. For a given
502 selection coefficient, we have shown that the long-term impact on disease is negligible for variants that
503 are more immune evasive, but only transiently so, eliciting variant-specific antibodies that protect from
504 reinfection (Figure 5A). By contrast, immune evasive variants that fail to elicit variant-specific
505 antibodies have a persistent advantage, leading to a nearly proportional increase in cases in the long term
506 (Figure 5B). In Appendix 2, we also consider variants that cause immunity to become leakier, increasing
507 the risk of infection for all recovered classes, which are particularly problematic (Figure S3), causing a
508 high long-term rise in cases because all individuals remain prone to infection if leakiness is persistent.
509 Variants that are more transmissible generally have an intermediate impact on disease incidence (Figure
510 5C). Thus, depending on the exact properties of new variants, we may see smaller or larger rises in cases
511 over the long term, even for variants initially spreading at the same rate.

512 Lab assays of SARS-CoV-2 have dramatically sped up phenotypic assessment of new variants (Cao et
513 al. 2023). Within days of new variants emerging, information has been shared by groups around the
514 world, evaluating immune evasiveness (e.g., the titer of neutralizing antibodies in convalescent plasma
515 required to prevent infection of cell lines) and efficiency of binding to ACE-2 receptors (e.g., via twitter,
516 @yunlong_cao). These assays often find that infection with one variant (e.g., BA.1) builds higher
517 neutralizing capacity against that variant than other variants (e.g., BA.2), indicating some loss of
518 immune evasiveness following infection with a variant (Cao et al. 2023). The impact on long-term
519 immune evasion and reinfection rates for different variants remains an open question, and one whose
520 answer determines the impact on endemic incidence of disease (Figure 5A,B).

521 We can counter variant-induced rises in cases, however, by encouraging higher uptake rates of vaccines
522 and other non-pharmaceutical interventions. These measures always help individuals reduce their own
523 risk of infection and the risk of infecting those around them (Figure 7). Widespread, but not universal,
524 uptake is needed to substantially reduce levels of disease (Figure 8), except if the disease is near
525 eradication (\tilde{R}_0 near 1). The benefits could be enhanced by encouraging NPI measures around those who
526 are most at risk of adverse outcomes and in places and times where risks of infection and/or the health
527 care burden are high. Particularly valuable are investments in measures that protect all, regardless of
528 uptake (such as improved air filtration and ventilation, adequate testing and job security to stay home
529 when sick).

530 The models explored herein lack many important epidemiological details, including spatial and age
531 structure in contact rates and seasonal variation in transmission risk. As such, the results are meant to
532 guide expectations rather than provide precise predictions. Details were sacrificed in an effort to help us
533 better understand how the endemic level of disease is likely to change in the future, in response to our
534 efforts as well as further evolution of the virus.

535 **Supplementary Materials (FOR REVIEW)**

536 All proofs and code needed to generate the figures are available in *Mathematica* and PDF versions at
537 <https://www.zoology.ubc.ca/~otto/Research/Endemic> (to be deposited in Dryad).

538 **Acknowledgements**

539 We thank all the authors, developers, and contributors to the VirusSeq database for making their
540 SARS-CoV-2 sequences publicly available. We thank especially the Canadian Public Health Laboratory
541 Network, academic sequencing partners, diagnostic hospital labs, and other sequencing partners for the
542 provision of the Canadian sequence data used in Figure 1. The authors would like to thank the scientific
543 community of the Coronavirus Variants Rapid Response Network (CoVaRR-Net), particularly Fiona
544 Brinkman, Carmen Lia Murall, Jesse Shapiro, and Justin Yue for helpful discussions about variants.
545 Funding was provided by the Natural Sciences and Engineering Research Council of Canada to SPO
546 (RGPIN- 2022-03726), to AM (RGPIN-2022-03113), and to CC (CANMOD; RGPIN-2019-06624), by
547 the Canada Research Chairs Program (SPO and AM) and the Canada 150 Research Chair Program (CC),
548 and by the Canadian Institutes for Health Research (CIHR) operating grant to CoVaRR-Net.

549
550 **Declaration of Interests**

551 The authors declare no competing interests.

552 **Appendix 1: Modelling the spread of variants**

553 *Dynamics* – We include infections by a resident variant (I) and a new variant (I^*) in the SIR_n
 554 epidemiological model illustrated in Figure 1. By allowing for multiple recovered classes, we can model
 555 new variants that are more immune evasive by allowing them to infect earlier in the waning period
 556 (infecting individuals in the last m recovered compartments R_j), when antibody levels are high enough
 557 to prevent infection by the resident virus but not the new variant. The dynamics are then described by
 558 the following set of differential equations:

$$\begin{aligned}
 559 \quad \frac{dS}{dt} &= \delta_n R_n - \beta SI - \beta^* SI^* \\
 560 \quad \frac{dI}{dt} &= \beta SI - \kappa I & \frac{dI^*}{dt} &= \beta^* (S + \sum_{j=1+n-m}^n R_j) I^* - \kappa I^* & (A1) \\
 561 \quad \frac{dR_1}{dt} &= \kappa I + \kappa I^* - \delta_1 R_1 \\
 562 \quad \frac{dR_j}{dt} &= \delta_{j-1} R_{j-1} - \delta_j R_j & & \text{for } 2 \leq j \leq n - m \\
 563 \quad \frac{dR_j}{dt} &= \delta_{j-1} R_{j-1} - \delta_j R_j - \beta^* R_j I^* & & \text{for } n - m < j \leq n
 \end{aligned}$$

564 Setting all waning rates between recovered classes equal to $\delta_i = \delta/n$ ensures that the average time from
 565 first recovering to returning to the susceptible class has a mean of $1/\delta$ days. The distribution of waning
 566 times is then given by a gamma distribution with a coefficient of variation (CV) of $1/\sqrt{n}$, becoming
 567 more bell shaped with higher n (Hethcote, Stech, and Van Den Driessche 1981).

568 *Spread of a new variant* – The spread of a new variant into a population at the stable endemic
 569 equilibrium (equation (2)) is given by the leading eigenvalue, λ_L of the external stability matrix
 570 describing the dynamics of the variant (see details in the Supplementary *Mathematica* package), which
 571 equals:

$$572 \quad \lambda_L = \hat{S}\beta^* + m\hat{R}_j\beta^* - \kappa \quad (A2)$$

573 If the new variant did not change the transmission rate ($\beta^* = \beta$) and was unable to infect any additional
 574 sector of the population ($m = 0$), it would be neutral ($\lambda_L = 0$, plugging in (2)).

575 The selection coefficient favouring a new variant is defined by the rise in frequency of the new variant
 576 relative to the old variant ($\frac{dx}{dt} \equiv s x$, where $x = \text{freq}(\text{new variant})/\text{freq}(\text{old variant})$), which predicts an
 577 exponential rise in the relative frequency of the new variant over time ($x_t = e^{st} x_0$). The strength of
 578 selection can thus be estimated empirically by the slope on a logit plot (plotting log of x_t over time).
 579 Near the endemic equilibrium, it can be shown that selection, defined in this way, equals λ_L (see
 580 Supplementary *Mathematica* package). Plugging in equation (2) for \hat{S} into (A2) then gives the selection
 581 coefficient reported in equation (4).

582 *Parameter values* – We consider the following parameter values for the current endemic phase during
 583 which Omicron predominates, giving the nominal value considered typical and the plausible range in
 584 square brackets:

- 585 • κ of 0.2 (mean of 5 days) [range of 3-10 days]. Source: Estimates of the infectious period for
 586 Omicron vary depending on the study design, but several studies are consistent with
 587 infectiousness for a couple of days prior to symptom onset and five days thereafter (UKHSA
 588 2023). We take into account some self-isolation upon infection and use a five-day average
 589 infectious period as a default.
- 590 • δ of 0.008 (mean of 125 days) [range of 100-180 days]. Source: Waning rate depends on the
 591 exact sequence of vaccinations and infections. The half-life of protection against symptomatic
 592 infection with Omicron among studies summarized by Menegale et al. (Menegale et al. 2023)
 593 was 87 days without a booster and 111 days with a booster, yielding δ values ranging from
 594 0.0071 to 0.0094 per day. Waning rates were similar for older and younger individuals
 595 (Menegale et al.’s eFigure 14).
- 596 • \hat{I} of 2% [range of 0.5%-4%]. Sources: The last report of the Coronavirus (COVID-19) Infection
 597 Survey UK (Office for National Statistics 2023), which assayed nose and throat swabs from
 598 households, found 2.66% of England were infected (13 March 2023). In Canada, models suggest
 599 that 1 in 28 were infected the week of 16 April 2023, while 1 in 80 were infected the week of 9
 600 September 2023 (COVID-19 Resources Canada 2023).
- 601 • Age structure for Canada: 13% of the population is 70+ in age (Statistics Canada 2023).

602 Combining these estimates with equations (2) and (3) allows estimation of the transmission rate and
 603 reproductive number. The nominal parameters given above yield estimates of $\beta = 0.42$ and $\tilde{R}_0 = 2.1$,
 604 ranging from $\beta = \{0.11-2.27\}$ and $\tilde{R}_0 = \{1.1,6.8\}$ (Table S1), although some combinations are not
 605 possible (e.g., a mean waning time of 180 days is inconsistent with an incidence of $\hat{I} = 4\%$ if mean
 606 clearance times are too short, $\kappa > 0.13$), and the disease is then expected to decline.

607 The expected number of disease bouts per year is 1.46 for the nominal parameter values, ranging from 0
 608 (when the disease disappears) to 2.92 when incidence is high ($\hat{I} = 4\%$), waning is fast ($\delta = 1/100$), and
 609 recovery is fast but not so fast that the disease disappears ($\kappa = 1/5$).

610 We can also calculate the expected number of infections per year for an individual who is vaccinated at
 611 regular intervals (every T days). For simplicity, we make the approximation that vaccinations are
 612 frequent enough and waning slow enough that we need only consider the chance of one infection
 613 between vaccinations. If waning times were exponentially distributed, then the probability of becoming
 614 infected in the period between vaccinations would be:

$$\begin{aligned}
 615 \quad P &= \int_0^T \underbrace{\delta e^{-\delta t}}_{\text{Waning at time } t} * \underbrace{(1 - e^{-\beta \hat{I}(T-t)})}_{\text{Probability of infection after waning}} dt & (A3) \\
 616 \quad &= 1 - \frac{e^{-\delta T} \beta \hat{I} - e^{-\beta \hat{I} T} \delta}{\beta \hat{I} - \delta}.
 \end{aligned}$$

617 The approximate annual number of infections is then $365 P/T$, which is 0.88 for those on a six-month
 618 vaccination interval ($T = 365/2$) and the nominal parameter values ($\kappa = 0.2$, $\delta = 0.008$, $\hat{I} = 2\%$, $\beta =$
 619 0.42).

620

621 **Appendix 2: Model sensitivity and oscillatory behaviour**

622 Different choices about the number of recovered classes, movement among them, and whether immunity
623 is leaky, as well as the inclusion of a latent period and incomplete seroconversion, were explored to
624 determine sensitivity of the results to model assumptions (Supplementary *Mathematica* file). To
625 simplify the presentation, we focus on the case where daily vaccination rates are low and are ignored
626 (except where noted).

627 *Alternate models of recovery* – In the main text, we used multiple recovered classes in the SIR_n model to
628 capture observed declines in neutralizing antibodies, measured on a log scale, over time since
629 vaccination and/or infection. While this reflects the dynamics of neutralizing antibody levels, a side
630 consequence is that the distribution for the total waning time becomes increasingly bell shaped as n rises
631 (CV of $1/\sqrt{n}$). This synchronizes the recovery of individuals infected at the same time. If n is large
632 enough, this synchronisation can destabilize the endemic equilibrium, leading to persistent cycles
633 (Hethcote, Stech, and Van Den Driessche 1981). While the rise in frequency of a variant, as described
634 by its selective advantage (equation (4)) and the long-term impact of the variant on the endemic
635 equilibrium (equation (5)) are insensitive to the number of recovered compartments (n), the extent of
636 oscillations following the initial spread of the variant are much stronger as n increases (Figure S2, panels
637 A-C). Empirically, the distribution of waning times is close to exponential (CV = 1; (Menegale et al.
638 2023)), suggesting that intrinsic oscillations are likely to be damped (like Figure S2A, where CV = 1).

639 Similar behaviour to Figure S2A is seen in a model with only two recovered classes ($n = 2$),
640 corresponding to high (R_1) and low (R_2) antibody levels, where an immune evasive variant (but not the
641 resident virus) can infect the second class. By setting the waning rates to $\delta_1 = \delta/x$ (from R_1 to R_2) and
642 $\delta_2 = \delta/(1 - x)$ (from R_2 to S), the equilibrium fraction of recovered individuals in the second class (x)
643 can be adjusted to allow for more immune evasive variants, while keeping the average time from first
644 recovering to susceptibility at $1/\delta$ days for the resident virus. This model has a nearly exponential
645 waning time, with rapidly dampening oscillations, for more transmissible variants (Figure S2D), more
646 immune evasive variants (Figure S2E), or both (Figure S2F). The selection coefficient and equilibrium
647 remain unchanged, all else being equal (given by equations (4) and (5), respectively).

648 *Leaky immunity* – In the main text, we considered immunity to be polarized: individuals are either
649 susceptible to infection (S compartment) or not (R_j compartments, with j depending on the variant).
650 There is evidence, however, that SARS-CoV-2 immunity is leaky, such that high viral exposure can lead
651 to infection for those who would otherwise be immune (Lind et al. 2023). Furthermore, variants may
652 differ in the extent of leaky immune (e.g., (Lind et al. 2023) found higher hazard ratios following close
653 exposure for Delta than for Omicron).

654 We thus explored variants that increased leakiness of immunity, ξ , in the SIR ($n = 1$) and SIR_n ($n = 5$)
655 models (exploring the latter numerically only in the Supplementary *Mathematica* file). Incorporating
656 leaky immunity in the SIR model changes the dynamics to:

657
$$\frac{dS}{dt} = \delta R - \beta SI - \beta^* SI^*$$

$$658 \quad \frac{dI}{dt} = \beta SI + \xi \beta RI - \kappa I \quad \frac{dI^*}{dt} = \beta^* S I^* + \xi^* \beta^* R I^* - \kappa I^* \quad (A4)$$

$$659 \quad \frac{dR}{dt} = \kappa I + \kappa I^* - \xi \beta RI - \xi^* \beta^* R I^* - \delta R$$

660 The equilibrium is then:

$$661 \quad \hat{S} = \frac{1}{2}(-b + \sqrt{b^2 - 4c})$$

$$662 \quad \hat{I} = \frac{\delta \left(\frac{\kappa}{\beta} - \hat{S}\right)}{\hat{S} \xi \beta} \quad (A5)$$

663 where $b = -\frac{\kappa - \delta - \xi \beta}{(1 - \xi)\beta}$ and $c = -\frac{\kappa}{\beta} \frac{\delta}{(1 - \xi)\beta}$. Selection on a variant then becomes:

$$664 \quad s = \underbrace{\frac{\Delta \beta}{\beta} \kappa}_{\text{Transmission advantage}} + \underbrace{\Delta \xi \hat{R} \beta^*}_{\text{Evasion advantage}} \quad (A6)$$

665 Figure S3 illustrates cases where immunity was robust against the resident virus ($\xi = 0$) but leaky for
 666 the variant ($\xi^* > 0$), combined with some to no transmission advantage (panels A to C). Again we see
 667 that the same selective advantage (s) is consistent with substantially different long-term consequences
 668 for endemic disease levels. Variants that exhibit leakier immunity greatly increase the endemic
 669 equilibrium, more than seen in Figures 3 and 4 for a given selection coefficient, because all individuals
 670 are more prone to infection in the long term, not just those with low antibody levels.

671 *Latent period* – Viral infections are characterized by a latent period between infection and detectable
 672 viral load, which is thought to indicate the onset of the infectious period (UKHSA 2023). We can
 673 include this period by adding to the SIR_n model a latent class (E), into which all new infections enter and
 674 then exit at rate ϵ . Including this period, the equilibrium fraction of infected individuals changes to:

$$675 \quad \hat{I} = \left(1 - \frac{\kappa}{\beta}\right) \frac{\delta \epsilon}{\epsilon \delta + \epsilon \kappa + \delta \kappa} \quad (A7)$$

676 Given that the rate of leaving the latent class is much faster than waning ($\epsilon \gg \delta$), the last $\delta \kappa$ term in the
 677 denominator is negligible, and ϵ cancels out of (A7). Thus, the equilibrium number of infections (\hat{I}) is
 678 nearly unaffected by including a latent class.

679 Recalculating the leading eigenvalue at this endemic equilibrium, the selection coefficient favoring the
 680 new variant ($s = \lambda_L$) changes slightly when a latent period is added, from s given by equation (4) to:

$$681 \quad s = -\frac{\epsilon + \kappa}{2} + \sqrt{\left(\frac{\epsilon + \kappa}{2}\right)^2 + s \epsilon} \quad (A8)$$

682 Assuming that the spread of the variant is slow relative to the latent and infectious periods ($s \ll \epsilon, \kappa$),
 683 adding a latent period causes selection to weaken slightly, with (A8) approaching $s \frac{1}{1 + \kappa/\epsilon}$. This occurs
 684 because only during a fraction $\frac{1/\kappa}{1/\epsilon + 1/\kappa} = \frac{1}{1 + \kappa/\epsilon}$ of the generation time of the virus is it infectious. Xin et
 685 al. (Xin et al. 2023) estimate a mean latent period of 3.1 days for Omicron. For the parameters

686 considered typical of Omicron (Appendix 1), selection would be ~70% as strong with a latent period.
 687 We ignore this correction to simplify the model presentation.

688 *Seroconversion* – Another real-world complication is that not all individuals seroconvert following
 689 infection or vaccination (i.e., not all infections elicit a robust immune response). If a fraction q of
 690 infections boost immunity (meaning here that they recover to the R_1 compartment in the SIR_n model),
 691 while $1-q$ return become susceptible again (returning to the S compartment), the equilibrium fraction of
 692 infected individuals changes to:

$$693 \quad \hat{I} = \left(1 - \frac{\kappa}{\beta}\right) \frac{\delta/q}{\delta/q + \kappa}. \quad (\text{A9})$$

694 Thus, decreasing the seroconversion rate by a factor q has the same effect on the endemic equilibrium as
 695 increasing the waning rate by a factor $1/q$ (equation (5)), and the same holds for the selection coefficient
 696 of a variant, s (equation (4), supplementary *Mathematica* file). The temporal dynamics of the wavelets
 697 are slightly different, with immediate waning for those who do not seroconvert and slower waning for
 698 those who do (supplementary *Mathematica* file).

699 Seroconversion rates for vaccines can also be included, changing the equilibrium to:

$$700 \quad \hat{I} = \left(1 - \frac{\kappa}{\beta}\right) \frac{\delta/q}{\delta/q + \kappa} - \frac{v q_v/q}{\delta/q + \kappa}. \quad (\text{A9})$$

701 where q_v is the seroconversion rate for vaccination (here meaning the probability that a vaccine dose
 702 boosts antibodies and provides protection from infection). If seroconversion rates are similar following
 703 infection and vaccination ($q_v = q$), then the results for selection (equation (3)) and endemic incidence
 704 (equation (4)) are again the same if we replace δ (ignoring seroconversion) with δ/q (including it).

705 To simplify the presentation, we do not explicitly include seroconversion but consider a range of waning
 706 rates to cover both seroconversion and waning.

707 Empirically, high seroconversion rates have been reported following vaccination with a single dose of
 708 Pfizer's BNT162b2 ($q = 99.5\%$) or AstraZeneca ChAdOx1 ($q = 97.1\%$), leading to antibodies
 709 recognizing the spike protein (Wei et al. 2021). Slightly lower seroconversion ($q = 93.5-95.3\%$) was
 710 observed following infection in early 2020 (Oved et al. 2020). An estimate following Omicron infection
 711 inferred even lower rates of seroconversion of $q = 74-81\%$ (here examining antibodies to nucleocapsid,
 712 as anti-spike antibodies were nearly universal in the highly vaccinated population examined; (Erikstrup
 713 et al. 2022)).

714 **Appendix 3: Non-pharmaceutical interventions**

715 We consider an expansion of the SIR_n epidemiological model to allow heterogeneity in behaviour. As
 716 illustrated in Figure S4, we now allow two classes of individuals, those who regularly adhere to stronger
 717 NPI measures, such as masking (indicated by an ‡), and those who do not:

$$718 \quad \frac{dS}{dt} = \delta_n R_n - \beta SI - (1-p)\beta SI^\ddagger \quad \frac{dS^\ddagger}{dt} = \delta_n R_n^\ddagger - (1-p)\beta S^\ddagger I - (1-p)^2 \beta S^\ddagger I^\ddagger$$

$$719 \quad \frac{dI}{dt} = \beta SI + (1-p)\beta SI^\ddagger - \kappa I \quad \frac{dI^\ddagger}{dt} = (1-p)\beta S^\ddagger I + (1-p)^2 \beta S^\ddagger I^\ddagger - \kappa I^\ddagger \quad (\text{A10})$$

$$720 \quad \frac{dR_1}{dt} = \kappa I - \delta_1 R_1 \qquad \frac{dR_1^\ddagger}{dt} = \kappa I^\ddagger - \delta_1 R_1^\ddagger$$

$$721 \quad \frac{dR_j}{dt} = \delta_{j-1} R_{j-1} - \delta_j R_j \qquad \frac{dR_j^\ddagger}{dt} = \delta_{j-1} R_{j-1}^\ddagger - \delta_j R_j^\ddagger \qquad \text{for } 2 \leq j \leq n$$

722

723 where the last line of equations is repeated for the remaining waning classes (j from 2 to n). We again
 724 set all rates between waning classes to $\delta_i = \delta/n$ (mean waning time of $1/\delta$ days). The new parameter p
 725 measures the protection provided when one individual in an interaction engages in NPI measures
 726 (reducing β by a factor $1-p$). If both infected and susceptible individuals uphold these measures,
 727 transmission is reduced by $(1-p)^2$. All variables are measured as proportions of the total population,
 728 with f being the fraction of the population carrying out NPI measures, such as masking (the sum of the \ddagger
 729 variables).

730 There are two equilibria of this system (A10), one where the disease is absent and one where the disease
 731 is endemic at:

$$732 \quad \hat{S} = \frac{1}{2}(-B + \sqrt{B^2 - 4C}) \qquad \hat{S}^\ddagger = \frac{\kappa - \beta \hat{S}}{(1-p)^2 \beta}$$

$$733 \quad \hat{I} = (1 - f - \hat{S}) \frac{\delta}{\delta + \kappa} \qquad \hat{I}^\ddagger = (1 - f - \hat{S}) \frac{\delta}{\delta + \kappa} \frac{\kappa - \beta \hat{S}}{(1-p) \beta \hat{S}} \qquad (\text{A11})$$

$$734 \quad \hat{R}_j = \hat{R}_{j-1} = \frac{1 - f - \hat{S} - \hat{I}}{n} \qquad \hat{R}_j^\ddagger = \hat{R}_{j-1}^\ddagger = \frac{f - \hat{S} - \hat{I}}{n} \qquad \text{for } 1 \leq j \leq n$$

735

736 where $B = \frac{(1-f)(1-p)\beta + f(1-p)^2\beta - \kappa p}{p\beta}$ and $C = -\frac{(1-f)(1-p)\kappa}{p\beta}$. The disease-absent equilibrium is locally
 737 stable when transmission rates are low relative to clearance, such that the endemic reproductive number
 738 if everyone were susceptible is less than one, $\tilde{R}_0 = \frac{(1-f)\beta + f(1-p)^2\beta}{\kappa} < 1$, in which case the endemic
 739 equilibrium does not exist (i.e., not all variables are positive). Otherwise, when $\tilde{R}_0 > 1$, the endemic
 740 equilibrium exists and is stable for the parameters considered, but it may become unstable for large n
 741 (Hethcote, Stech, and Van Den Driessche 1981).

742 At this equilibrium, the risk that an individual is in the infected class at any point in time is \hat{I}^\ddagger/f if they
 743 regularly mask and $\hat{I}/(1-f)$ if they do not, from which we calculate the relative risk in the main text.
 744 The population-level impact of NPI measures, such as masking, is determined by analysing the fraction
 745 of the population expected to be infected at any point in time, $\hat{I} + \hat{I}^\ddagger$.

746 The above assumes that an individual's choice about engaging in NPI measures remains constant over
 747 time, but we also consider the opposite case (detailed in the Supplementary *Mathematica* file), where
 748 individuals rapidly switch between engaging or not in NPI measures. Assuming that the behaviour
 749 persists over the short time frame of an infection but that individuals switch often while in the longer
 750 susceptible or recovered phases, we can simplify the model by monitoring only those engaging in NPI
 751 measures at the time of exposure, with f then representing the probability that an individual engages in

752 the NPI measures at that time. We thus only sub-divide the infectious class into those who were or were
 753 not practicing the NPI measures at the time of infection (I^\ddagger or I , respectively). The dynamics are then:

$$754 \quad \frac{dS}{dt} = \delta_n R_n - (1-f)\beta SI - (1-p)f\beta SI - (1-p)(1-f)\beta SI^\ddagger - (1-p)^2 f\beta SI^\ddagger \quad (\text{A12})$$

$$755 \quad \frac{dI}{dt} = (1-f)\beta SI + (1-p)(1-f)\beta SI^\ddagger - \kappa I \quad \frac{dI^\ddagger}{dt} = (1-p)f\beta SI + (1-p)^2 f\beta SI^\ddagger - \kappa I^\ddagger$$

$$756 \quad \frac{dR_1}{dt} = \kappa I + \kappa I^\ddagger - \delta_1 R_1$$

$$757 \quad \frac{dR_j}{dt} = \delta_{j-1} R_{j-1} - \delta_j R_j \quad \text{for } 2 \leq j \leq n$$

758 Results using (A12) instead of (A10) are similar, except that practicing and non-practicing individuals
 759 are equally likely to be susceptible at the time of exposure, so that the individual-level protective effect
 760 of the NPI measure now depends only on p and not on \tilde{R}_0 , as discussed in the text.

761 *Parameters:* The protection (p) and uptake (f) depend on the NPI measure considered (The Royal
 762 Society 2023). Here we briefly review data on masking as a protective measure. One metaanalysis of
 763 randomized control studies prior to the COVID-19 pandemic found protection provided by masks was p
 764 = 16% for respiratory infections, rising to $p = 24\%$ in studies longer than two weeks (Li et al. 2022).
 765 Importantly, many individual studies were underpowered but the results were consistent across studies
 766 (see Figure 2 in Li et al. 2022).

767 For COVID-19, a metaanalysis of the impact of mask mandates estimated a 25% reduction in
 768 transmission rates, comparing transmission levels predicted if everyone were in the class that self-report
 769 wearing masks “most of the time in some public places” to that if no one wore masks (Leech et al.
 770 2022). Importantly, the authors showed that the lifting or imposition of mandates rarely had dramatic
 771 immediate effects on mask wearing, emphasizing that mandates are a poor proxy for mask wearing.
 772 Their analysis thus benefited from a global analysis of trends in mask-wearing behavior around the time
 773 of mandates by incorporating data from a survey of masking behaviour among nearly 20 million
 774 individuals.

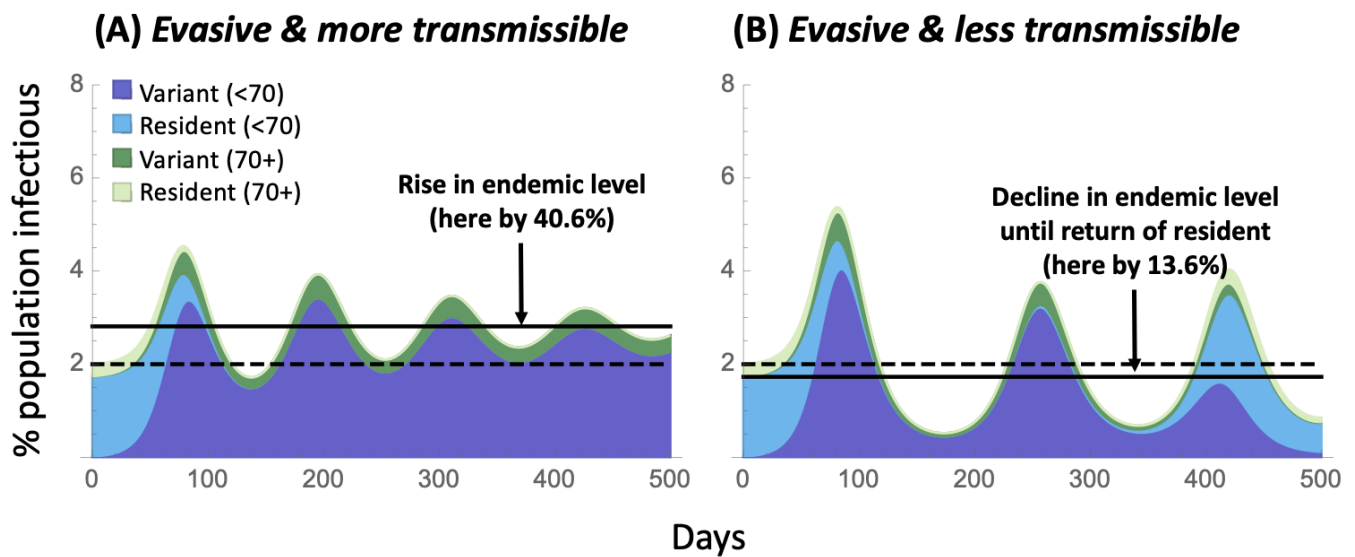
775 As argued by Leech et al. (2022), this effect size is likely to be underestimated for a number of reasons.
 776 First, the study period (1 May – 1 September 2020) occurred when cloth masks predominated, because
 777 high-quality masks were largely unavailable outside of health care settings. Second, the definition of
 778 mask use was broad and included individuals who only occasionally mask and do so in few public
 779 places. We thus consider that $p = 0.25$ represents a lower bound on the protection provided by masking.

780 Higher values are plausible when using high-quality masks and doing so consistently in indoor public
 781 spaces. For example, masks provided a stronger benefit, reducing the odds ratio of infection by an
 782 average of 50% among the studies summarized within healthcare settings (The Royal Society 2023). We
 783 thus consider $p = 0.5$ to represent a reasonable upper bound on the protection provided by masking
 784 attainable by consistent wearing of high-quality masks. Combinations of NPI measures, including
 785 improved ventilation, avoiding crowded indoor environments, testing and self-isolation, and masking
 786 may provide considerably stronger protection.

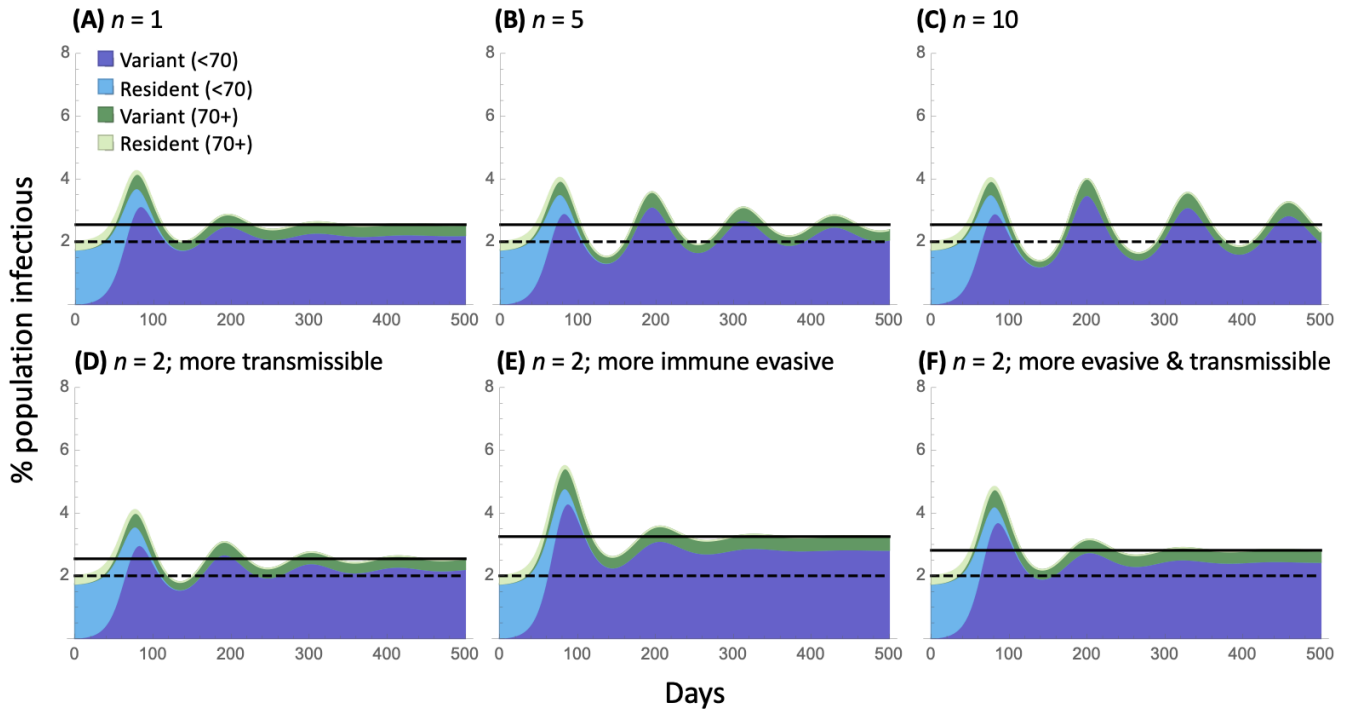
787 **Table S1: Parameter estimates and inferred rates.** The first three columns are estimated from the
788 literature (Appendix 1). Using equation (2), these parameters provide estimates for the transmission rate
789 (β), the endemic reproductive number ($\tilde{R}_0 = \beta/\kappa$), the fraction of susceptible individuals (\hat{S}), and the
790 estimated annual number of infections at the endemic equilibrium (inferred values are in italics). The
791 first row gives the nominal parameter values used in the text. “NA” are parameter combinations that do
792 not sustain an endemic equilibrium of the disease. Estimates are given without ongoing vaccination ($v =$
793 0) but are nearly identical with low rates, as in Canada during the summer of 2023 ($v = 0.00012$, all
794 differences $<12\%$; see supplementary *Mathematica* file for estimates with higher rates of vaccination).

Incidence (\hat{I})	Waning rate (δ)	Recovery rate (κ)	Transmission rate (β)	Reproductive number (\tilde{R}_0)	Susceptible (\hat{S})	Annual # of infections
0.02	0.008	0.2	<i>0.417</i>	<i>2.083</i>	<i>0.48</i>	<i>1.46</i>
0.02	0.008	0.333	<i>2.273</i>	<i>6.818</i>	<i>0.147</i>	<i>2.433</i>
0.02	0.008	0.1	<i>0.137</i>	<i>1.37</i>	<i>0.73</i>	<i>0.73</i>
0.02	0.01	0.2	<i>0.345</i>	<i>1.724</i>	<i>0.58</i>	<i>1.46</i>
0.02	0.01	0.333	<i>1.064</i>	<i>3.191</i>	<i>0.313</i>	<i>2.433</i>
0.02	0.01	0.1	<i>0.128</i>	<i>1.282</i>	<i>0.78</i>	<i>0.73</i>
0.02	0.006	0.2	<i>0.769</i>	<i>3.846</i>	<i>0.26</i>	<i>1.46</i>
0.02	0.006	0.333	NA	NA	NA	NA
0.02	0.006	0.1	<i>0.161</i>	<i>1.613</i>	<i>0.62</i>	<i>0.73</i>
0.005	0.008	0.2	<i>0.23</i>	<i>1.149</i>	<i>0.87</i>	<i>0.365</i>
0.005	0.008	0.333	<i>0.424</i>	<i>1.271</i>	<i>0.787</i>	<i>0.608</i>
0.005	0.008	0.1	<i>0.107</i>	<i>1.072</i>	<i>0.932</i>	<i>0.182</i>
0.005	0.01	0.2	<i>0.223</i>	<i>1.117</i>	<i>0.895</i>	<i>0.365</i>
0.005	0.01	0.333	<i>0.402</i>	<i>1.207</i>	<i>0.828</i>	<i>0.608</i>
0.005	0.01	0.1	<i>0.106</i>	<i>1.058</i>	<i>0.945</i>	<i>0.182</i>
0.005	0.006	0.2	<i>0.245</i>	<i>1.227</i>	<i>0.815</i>	<i>0.365</i>
0.005	0.006	0.333	<i>0.48</i>	<i>1.439</i>	<i>0.695</i>	<i>0.608</i>
0.005	0.006	0.1	<i>0.11</i>	<i>1.105</i>	<i>0.905</i>	<i>0.182</i>
0.04	0.008	0.2	NA	NA	NA	NA
0.04	0.008	0.333	NA	NA	NA	NA
0.04	0.008	0.1	<i>0.217</i>	<i>2.174</i>	<i>0.46</i>	<i>1.46</i>
0.04	0.01	0.2	<i>1.25</i>	<i>6.25</i>	<i>0.16</i>	<i>2.92</i>
0.04	0.01	0.333	NA	NA	NA	NA
0.04	0.01	0.1	<i>0.179</i>	<i>1.786</i>	<i>0.56</i>	<i>1.46</i>
0.04	0.006	0.2	NA	NA	NA	NA
0.04	0.006	0.333	NA	NA	NA	NA
0.04	0.006	0.1	<i>0.417</i>	<i>4.167</i>	<i>0.24</i>	<i>1.46</i>

795



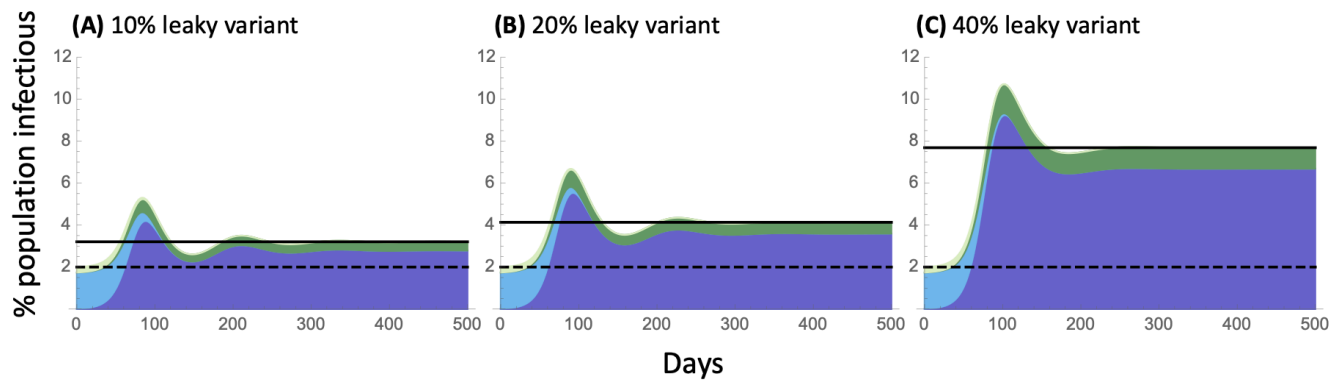
796 **FIGURE S1: Variants combining immune evasiveness and changes in transmissibility.** Panel A:
 797 Variant is persistently immune evasive (by half the amount shown in Figure 3B, able to infect $m = 1$ out
 798 of $n = 5$ recovered classes) and more transmissible (increasing β , and hence \tilde{R}_0 , by 17%). Panel B:
 799 Variant is even more immune evasive (50% more than in Figure 3B, able to infect $m = 3$ out of $n = 5$
 800 recovered classes) and less transmissible (decreasing β , and hence \tilde{R}_0 , by 17%), with immune evasion
 801 being transient. In both cases, β^* was chosen to give the variant the same selective advantage as in
 802 Figure 3 ($s = 8.3\%$), leading to the same initial rate of spread of the variant (dark shading) in a resident
 803 population of viruses (light shading). Because the variant is only transiently immune evasive in Panel B,
 804 the resident lineage, which is more transmissible, eventually takes over. Parameters: $\kappa = 0.2$, $\delta =$
 805 0.008 , $\hat{I} = 2\%$, $\beta = 0.42$. the nominal parameter estimates given in Appendix 1 for all age classes.



806

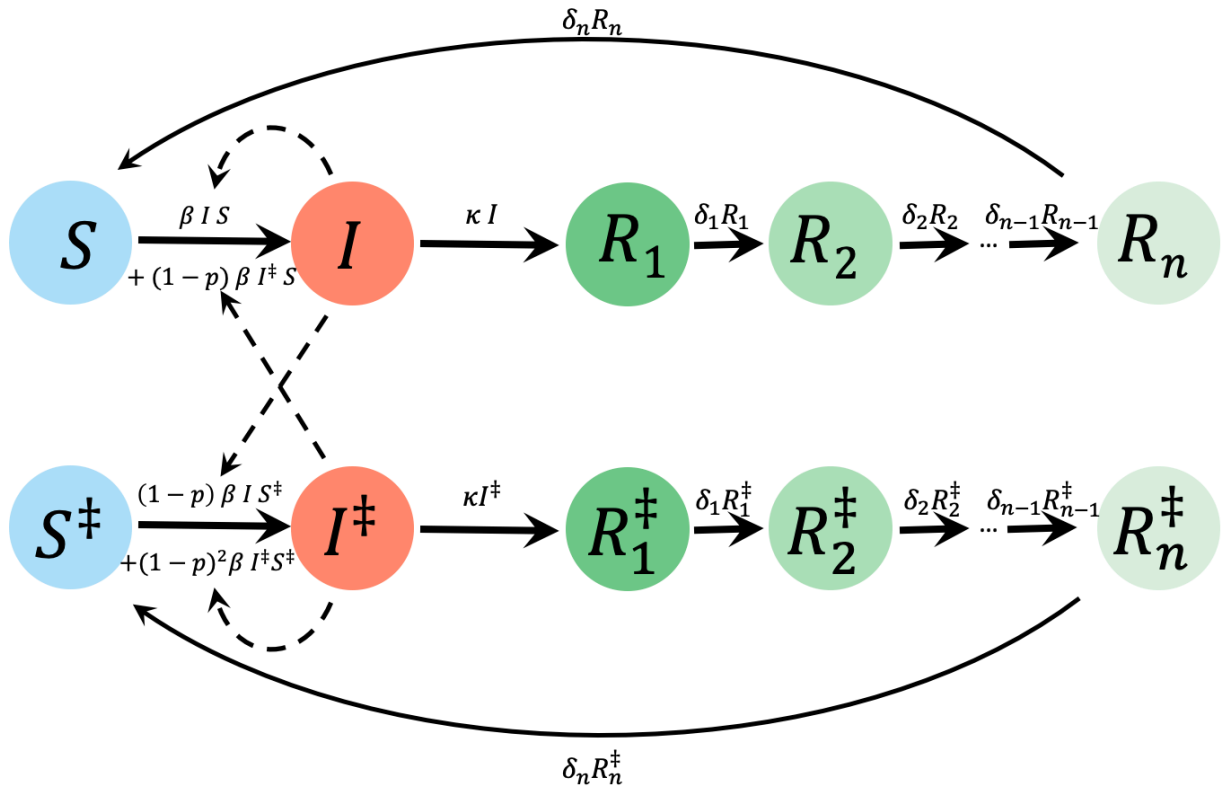
807 **FIGURE S2: Robustness to model structure.** Panels (A)-(C) illustrate the sensitivity of the dynamics
 808 to the number of recovery classes (n) for a more transmissible variant that increases β by 42% (panel B
 809 is equivalent to Figure 3). Holding the expected waning period constant at $1/\delta = 125$ days, increasing
 810 the number of compartments causes a more bell-shaped distribution of the waning period and increases
 811 oscillations following the spread of the variant (from panel A to C). Panels (D)-(F) consider two
 812 recovered compartments ($n = 2$), corresponding to high and low neutralizing antibody levels. At the
 813 endemic equilibrium, either 40% ($x = 0.4$; panels D, E) or 20% ($x = 0.2$, panel F) of recovered
 814 individuals are in the low-immunity compartment, which can be infected by a more immune evasive
 815 variant (panels E and F). The variant in panel (D) is only more transmissible. In each case, the
 816 transmissibility of the variant is adjusted to hold its selective advantage constant at ($s = 8.3\%$),
 817 increasing β by (A)-(D) 42%, (E) 0%, and (F) 17%. Parameters: $\kappa = 0.2$, $\delta = 0.008$, $\hat{I} = 2\%$, $\beta =$
 818 0.42 , the nominal parameter estimates given in Appendix 1 for all age classes.

819



820

821 **FIGURE S3: Robustness to model structure: allowing leaky immunity.** Panels illustrate the standard
 822 SIR model ($n = 1$) when variants increase leakiness of immunity. Individuals infectious with the variant
 823 can infect all recovered individuals with a transmission rate that is (A) $\xi = 10\%$, (B) 20% , and (C) 40%
 824 times β , whereas individuals carrying the resident virus can only infect susceptible individuals ($\xi = 0$).
 825 In each case, the transmissibility of the variant is adjusted to hold its selective advantage constant at $s =$
 826 8.3% , which required increasing β by (A) 28% , (B) 17% , and (C) 0% . Note that the y-axis has been
 827 increased relative to previous figures due to the greater long-term impact of variants able to infect all
 828 recovered classes by increasing the leakiness of immunity. Parameters: $\kappa = 0.2$, $\delta = 0.008$, $\hat{I} = 2\%$,
 829 $\beta = 0.42$, the nominal parameter estimates given in Appendix 1 for all age classes.



830

831 **FIGURE S4: Epidemiological model used to explore the benefits of NPI measures, such as**
 832 **masking.** We include behavioural heterogeneity in SIR_n model, where variables with a \ddagger denote
 833 individuals engaging in the NPI measure(s). As before, S are susceptible individuals, I are infectious,
 834 and R_n are recovered, with immunity at different stages of waning. The fraction of individuals engaging
 835 in NPI measures is $f = S^\ddagger + I^\ddagger + \sum_{i=1}^n R_i^\ddagger$. See Supplementary *Mathematica* file for an alternative
 836 model where individuals rapidly switch behaviours (switching between the upper and lower row of
 837 circles). Parameters are β : transmission rate, p : protection provided by masking (modeled as a reduction
 838 in transmission by a factor $(1-p)$ for each person in an interaction wearing a mask), κ : recovery rate, and
 839 δ_j : per-class waning rate.

840 **References [Format will be finalized following review]**

- 841 Andrews, Nick, Julia Stowe, Freja Kirsebom, Samuel Toffa, Tim Riekeard, Eileen Gallagher, Charlotte
842 Gower, et al. 2022. “Covid-19 Vaccine Effectiveness against the Omicron (B.1.1.529) Variant.”
843 *The New England Journal of Medicine* 386 (16): 1532–46.
- 844 Arabi, Maryam, Yousef Al-Najjar, Omna Sharma, Ibtihal Kamal, Aimen Javed, Harsh S. Gohil, Pradipta
845 Paul, Aljazi M. Al-Khalifa, Sa’ad Laws, and Dalia Zakaria. 2023. “Role of Previous Infection
846 with SARS-CoV-2 in Protecting against Omicron Reinfections and Severe Complications of
847 COVID-19 Compared to Pre-Omicron Variants: A Systematic Review.” *BMC Infectious*
848 *Diseases* 23 (1): 432.
- 849 Canadian Blood Services. 2023. “COVID-19 Seroprevalence Report July 28, 2023.” 2023.
850 [https://www.covid19immunitytaskforce.ca/wp-content/uploads/2023/08/covid-19-full-report-](https://www.covid19immunitytaskforce.ca/wp-content/uploads/2023/08/covid-19-full-report-june-2023.pdf)
851 [june-2023.pdf](https://www.covid19immunitytaskforce.ca/wp-content/uploads/2023/08/covid-19-full-report-june-2023.pdf).
- 852 Cao, Yunlong, Fanchong Jian, Jing Wang, Yuanling Yu, Weiliang Song, Ayijiang Yisimayi, Jing Wang,
853 et al. 2023. “Imprinted SARS-CoV-2 Humoral Immunity Induces Convergent Omicron RBD
854 Evolution.” *Nature* 614 (7948): 521–29.
- 855 CDC. 2023. “Stay Up to Date with COVID-19 Vaccines.” Stay Up to Date with COVID-19 Vaccines.
856 2023. <https://www.cdc.gov/coronavirus/2019-ncov/vaccines/stay-up-to-date.html>.
- 857 Chemaitelly, Hiam, Houssein H. Ayoub, Sawsan AlMukdad, Peter Coyle, Patrick Tang, Hadi M.
858 Yassine, Hebah A. Al-Khatib, et al. 2022. “Duration of mRNA Vaccine Protection against
859 SARS-CoV-2 Omicron BA.1 and BA.2 Subvariants in Qatar.” *Nature Communications* 13 (1):
860 3082.
- 861 CoVaRR-Net’s CAMEO. 2023. “Duotang, a Genomic Epidemiology Analyses and Mathematical
862 Modelling Notebook.” Duotang. 2023. <https://covarr-net.github.io/duotang/duotang.html>.
- 863 COVID-19 Resources Canada. 2023. “Detailed Forecasts: CAN, Followed by Each Province on
864 Subsequent Pages.” Detailed Forecasts: CAN, Followed by Each Province on Subsequent Pages.
865 2023. <https://covid19resources.ca/covid-hazard-index/>.
- 866 Day, Troy, Sylvain Gandon, Sébastien Lion, and Sarah P. Otto. 2020. “On the Evolutionary
867 Epidemiology of SARS-CoV-2.” *Current Biology: CB* 30 (15): R849–57.
- 868 Dorp, Christiaan H. van, Emma E. Goldberg, Nick Hengartner, Ruian Ke, and Ethan O. Romero-
869 Severson. 2021. “Estimating the Strength of Selection for New SARS-CoV-2 Variants.” *Nature*
870 *Communications* 12 (1): 7239.
- 871 Erikstrup, Christian, Anna Damkjær Laksafoss, Josephine Gladov, Kathrine Agergård Kaspersen, Susan
872 Mikkelsen, Lotte Hindhede, Jens Kjærgaard Boldsen, et al. 2022. “Seroprevalence and Infection
873 Fatality Rate of the SARS-CoV-2 Omicron Variant in Denmark: A Nationwide Serosurveillance
874 Study.” *The Lancet Regional Health. Europe* 21 (October): 100479.
- 875 Evans, John P., Cong Zeng, Claire Carlin, Gerard Lozanski, Linda J. Saif, Eugene M. Oltz, Richard J.
876 Gumina, and Shan-Lu Liu. 2022. “Neutralizing Antibody Responses Elicited by SARS-CoV-2
877 mRNA Vaccination Wane over Time and Are Boosted by Breakthrough Infection.” *Science*
878 *Translational Medicine* 14 (637): eabn8057.
- 879 Health Infobase Canada. 2023. “COVID-19 Vaccination: Doses Administered.” COVID-19
880 Vaccination: Doses Administered. 2023. [https://health-infobase.canada.ca/covid-19/vaccine-](https://health-infobase.canada.ca/covid-19/vaccine-administration/)
881 [administration/](https://health-infobase.canada.ca/covid-19/vaccine-administration/).
- 882 Hethcote, Herbert W., Harlan W. Stech, and P. Van Den Driessche. 1981. “Nonlinear Oscillations in
883 Epidemic Models.” *SIAM Journal on Applied Mathematics* 40 (1): 1–9.
- 884 Jacobsen, Henning, Ioannis Sitaras, Maeva Katzmarzyk, Viviana Cobos Jimenez, Robert Naughton,
885 Melissa M. Higdon, and Maria Deloria Knoll. 2023. “Waning of Post-Vaccination Neutralizing
886 Antibody Responses against SARS-CoV-2, a Systematic Literature Review and Meta-Analysis.”
887 *MedRxiv*. <https://doi.org/10.1101/2023.08.08.23293864>.

- 888 Keeling, Matt J., and Pejman Rohani. 2011. *Modeling Infectious Diseases in Humans and Animals*.
889 Princeton University Press.
- 890 Khoury, David S., Deborah Cromer, Arnold Reynaldi, Timothy E. Schlub, Adam K. Wheatley, Jennifer
891 A. Juno, Kanta Subbarao, Stephen J. Kent, James A. Triccas, and Miles P. Davenport. 2021.
892 “Neutralizing Antibody Levels Are Highly Predictive of Immune Protection from Symptomatic
893 SARS-CoV-2 Infection.” *Nature Medicine* 27 (7): 1205–11.
- 894 Lau, Chin Shern, May Lin Helen Oh, Soon Kieng Phua, Ya-Li Liang, and Tar Choon Aw. 2022. “210-
895 Day Kinetics of Total, IgG, and Neutralizing Spike Antibodies across a Course of 3 Doses of
896 BNT162b2 mRNA Vaccine.” *Vaccines* 10 (10). <https://doi.org/10.3390/vaccines10101703>.
- 897 Lau, Eric Hy, David Sc Hui, Owen Ty Tsang, Wai-Hung Chan, Mike Yw Kwan, Susan S. Chiu, Samuel
898 Ms Cheng, et al. 2021. “Long-Term Persistence of SARS-CoV-2 Neutralizing Antibody
899 Responses after Infection and Estimates of the Duration of Protection.” *EClinicalMedicine* 41
900 (November): 101174.
- 901 Leech, Gavin, Charlie Rogers-Smith, Joshua Teperowski Monrad, Jonas B. Sandbrink, Benedict Snodin,
902 Robert Zinkov, Benjamin Rader, et al. 2022. “Mask Wearing in Community Settings Reduces
903 SARS-CoV-2 Transmission.” *Proceedings of the National Academy of Sciences of the United
904 States of America* 119 (23): e2119266119.
- 905 Li, Hui, Kai Yuan, Yan-Kun Sun, Yong-Bo Zheng, Ying-Ying Xu, Si-Zhen Su, Yu-Xin Zhang, et al.
906 2022. “Efficacy and Practice of Facemask Use in General Population: A Systematic Review and
907 Meta-Analysis.” *Translational Psychiatry* 12 (1): 49.
- 908 Lin, Cheryl, Brooke Bier, Rungting Tu, John J. Paat, and Pikuei Tu. 2023. “Vaccinated Yet Booster-
909 Hesitant: Perspectives from Boosted, Non-Boosted, and Unvaccinated Individuals.” *Vaccines* 11
910 (3). <https://doi.org/10.3390/vaccines11030550>.
- 911 Lind, Margaret L., Murilo Dorion, Amy J. Houde, Mary Lansing, Sarah Lapidus, Russell Thomas, Inci
912 Yildirim, et al. 2023. “Evidence of Leaky Protection Following COVID-19 Vaccination and
913 SARS-CoV-2 Infection in an Incarcerated Population.” *Nature Communications* 14 (1): 5055.
- 914 Mahase, Elisabeth. 2023. “Covid-19: Annual Flu-like Booster Approach May Not Be Appropriate, Says
915 Expert on Infectious Disease.” *BMJ* 380 (January): 196.
- 916 Menegale, Francesco, Mattia Manica, Agnese Zardini, Giorgio Guzzetta, Valentina Marziano, Valeria
917 d’Andrea, Filippo Trentini, Marco Ajelli, Piero Poletti, and Stefano Merler. 2023. “Evaluation of
918 Waning of SARS-CoV-2 Vaccine-Induced Immunity: A Systematic Review and Meta-
919 Analysis.” *JAMA Network Open* 6 (5): e2310650.
- 920 NACI. 2023. “Guidance on the Use of COVID-19 Vaccines in the Fall of 2023.” Public Health Agency
921 of Canada. [https://www.canada.ca/content/dam/phac-
922 aspc/documents/services/publications/vaccines-immunization/national-advisory-committee-
923 immunization-guidance-use-covid-19-vaccines-fall-2023/statement.pdf](https://www.canada.ca/content/dam/phac-aspc/documents/services/publications/vaccines-immunization/national-advisory-committee-immunization-guidance-use-covid-19-vaccines-fall-2023/statement.pdf).
- 924 NHS. 2023. “About COVID-19 Vaccination.” About COVID-19 Vaccination. 2023.
925 <https://www.nhs.uk/conditions/covid-19/covid-19-vaccination/about-covid-19-vaccination/>.
- 926 Nyberg, Tommy, Neil M. Ferguson, Sophie G. Nash, Harriet H. Webster, Seth Flaxman, Nick Andrews,
927 Wes Hinsley, et al. 2022. “Comparative Analysis of the Risks of Hospitalisation and Death
928 Associated with SARS-CoV-2 Omicron (B.1.1.529) and Delta (B.1.617.2) Variants in England:
929 A Cohort Study.” *The Lancet* 399 (10332): 1303–12.
- 930 Office for National Statistics. 2023. “Results - Weekly Swab Positivity Updates from ONS.” Results -
931 Weekly Swab Positivity Updates from ONS. 2023.
932 [https://www.ons.gov.uk/peoplepopulationandcommunity/healthandsocialcare/conditionsanddisea
933 ses/bulletins/coronaviruscovid19infectionsurveypilot/24march2023](https://www.ons.gov.uk/peoplepopulationandcommunity/healthandsocialcare/conditionsanddiseases/bulletins/coronaviruscovid19infectionsurveypilot/24march2023).
- 934 Ogden, Nicholas H., Patricia Turgeon, Aamir Fazil, Julia Clark, Vanessa Gabriele-Rivet, Theresa Tam,
935 and Victoria Ng. 2022. “Counterfactuals of Effects of Vaccination and Public Health Measures

936 on COVID-19 Cases in Canada: What Could Have Happened?” *Canada Communicable Disease*
937 *Report = Relevé Des Maladies Transmissibles Au Canada* 48 (7–8): 292–302.

938 Otto, Sarah P., Troy Day, Julien Arino, Caroline Colijn, Jonathan Dushoff, Michael Li, Samir Mechai, et
939 al. 2021. “The Origins and Potential Future of SARS-CoV-2 Variants of Concern in the Evolving
940 COVID-19 Pandemic.” *Current Biology: CB* 31 (14): R918–29.

941 Our World in Data. 2023. “Our World in Data.” Daily COVID-19 Vaccine Doses Administered. 2023.
942 <https://ourworldindata.org/grapher/daily-covid-19-vaccination-doses>.

943 Oved, Kfir, Liraz Olmer, Yonat Shemer-Avni, Tamar Wolf, Lia Supino-Rosin, George Prajgrod, Yotam
944 Shenhar, et al. 2020. “Multi-Center Nationwide Comparison of Seven Serology Assays Reveals
945 a SARS-CoV-2 Non-Responding Seronegative Subpopulation.” *EClinicalMedicine* 29
946 (December): 100651.

947 Puhach, Olha, Kenneth Adea, Nicolas Hulo, Pascale Sattonnet, Camille Genecand, Anne Iten,
948 Frédérique Jacquérior, et al. 2022. “Infectious Viral Load in Unvaccinated and Vaccinated
949 Individuals Infected with Ancestral, Delta or Omicron SARS-CoV-2.” *Nature Medicine* 28 (7):
950 1491–1500.

951 Scherer, Almut, and Angela McLean. 2002. “Mathematical Models of Vaccination.” *British Medical*
952 *Bulletin* 62: 187–99.

953 Statistics Canada. 2023. “Population Estimates on July 1st, by Age and Sex.” Population Estimates on
954 July 1st, by Age and Sex. 2023.
955 <https://www150.statcan.gc.ca/t1/tb11/en/tv.action?pid=1710000501>.

956 Talic, Stella, Shivangi Shah, Holly Wild, Danijela Gasevic, Ashika Maharaj, Zanfina Ademi, Xue Li, et
957 al. 2021. “Effectiveness of Public Health Measures in Reducing the Incidence of Covid-19,
958 SARS-CoV-2 Transmission, and Covid-19 Mortality: Systematic Review and Meta-Analysis.”
959 *BMJ* 375 (November): e068302.

960 Tan, Sophia T., Ada T. Kwan, Isabel Rodríguez-Barraquer, Benjamin J. Singer, Hailey J. Park, Joseph
961 A. Lewnard, David Sears, and Nathan C. Lo. 2023. “Infectiousness of SARS-CoV-2
962 Breakthrough Infections and Reinfections during the Omicron Wave.” *Nature Medicine* 29 (2):
963 358–65.

964 The Royal Society. 2023. “COVID-19: Examining the Effectiveness of Non-Pharmaceutical
965 Interventions.” [https://royalsociety.org/-/media/policy/projects/impact-non-pharmaceutical-](https://royalsociety.org/-/media/policy/projects/impact-non-pharmaceutical-interventions-on-covid-19-transmission/the-royal-society-covid-19-examining-the-effectiveness-of-non-pharmaceutical-interventions-report.pdf)
966 [interventions-on-covid-19-transmission/the-royal-society-covid-19-examining-the-effectiveness-](https://royalsociety.org/-/media/policy/projects/impact-non-pharmaceutical-interventions-on-covid-19-transmission/the-royal-society-covid-19-examining-the-effectiveness-of-non-pharmaceutical-interventions-report.pdf)
967 [of-non-pharmaceutical-interventions-report.pdf](https://royalsociety.org/-/media/policy/projects/impact-non-pharmaceutical-interventions-on-covid-19-transmission/the-royal-society-covid-19-examining-the-effectiveness-of-non-pharmaceutical-interventions-report.pdf).

968 UKHSA. 2023. “COVID-19 Omicron Variant Infectious Period and Transmission from People with
969 Asymptomatic Compared with Symptomatic Infection: A Rapid Review.” GOV-14430. {UK
970 Health Security Agency}. [https://www.gov.uk/government/publications/covid-19-omicron-](https://www.gov.uk/government/publications/covid-19-omicron-variant-infectious-period-and-asymptomatic-and-symptomatic-transmission)
971 [variant-infectious-period-and-asymptomatic-and-symptomatic-transmission](https://www.gov.uk/government/publications/covid-19-omicron-variant-infectious-period-and-asymptomatic-and-symptomatic-transmission).

972 VirusSeq. 2023. “Canadian VirusSeq Data Portal.” Canadian VirusSeq Data Portal. 2023.
973 <https://virusseq-dataportal.ca/>.

974 Wei, Jia, Nicole Stoesser, Philippa C. Matthews, Daniel Ayoubkhani, Ruth Studley, Iain Bell, John I.
975 Bell, et al. 2021. “Antibody Responses to SARS-CoV-2 Vaccines in 45,965 Adults from the
976 General Population of the United Kingdom.” *Nature Microbiology* 6 (9): 1140–49.

977 Wichmann, Bruno, and Roberta Moreira Wichmann. 2023. “Big Data Evidence of the Impact of
978 COVID-19 Hospitalizations on Mortality Rates of Non-COVID-19 Critically Ill Patients.”
979 *Scientific Reports* 13 (1): 13613.

980 Xin, Hualei, Zhe Wang, Shuang Feng, Zhou Sun, Lele Yu, Benjamin J. Cowling, Qingxin Kong, and
981 Peng Wu. 2023. “Transmission Dynamics of SARS-CoV-2 Omicron Variant Infections in
982 Hangzhou, Zhejiang, China, January-February 2022.” *International Journal of Infectious*
983 *Diseases: IJID: Official Publication of the International Society for Infectious Diseases* 126
984 (January): 132–35.